

Three particle Pomeron and odderon states in QCD

Jan Koteński

M. Smoluchowski Institute of Physics, Jagellonian University
Reymonta 4, 30-059 Kraków, Poland

The scattering amplitude of hadrons in high energy Regge limit can be rewritten in terms of reggeized gluons, *i.e.* Reggeons. We consider three-Reggeon states that possess either $C = +1$ or $C = -1$ parity. In this work using Janik-Wosiek method the spectrum of conformal charges is calculated for states with conformal Lorentz spin $n_h = 0, 1, 2, 3, \dots$. Moreover corrections to WKB approximation are computed.

PACS numbers: 12.40.Nn, 11.55.Jy, 12.38.-t, 12.38.-t

Keywords: Reggeons, QCD, spectrum, eigenfunctions

TPJU-03/2006

1. Introduction

The reggeized gluon states, also called Reggeons, appear in scattering processes of Quantum Chromodynamics (QCD) in the Regge limit where the square of the total energy s is large while the transfer of four-momentum t is low and fixed. In this limit the leading contribution to the scattering amplitude of hadrons is dominated by the exchange of intermediate particles, Reggeons, which are the compound states of gluons [1, 2, 3, 4, 5, 6].

Even in the simplifying Regge limit in the generalized leading logarithm approximation [7, 8, 9] this problem is technically very complicated due to the non-abelian structure of QCD. Many Reggeon wave-functions are the eigenstates of a Hamiltonian which is equivalent in the 't Hooft's multi-colour limit [10, 11, 12] to the Hamiltonian for the non-compact Heisenberg $SL(2, \mathbb{C})$ spin magnet. Moreover, the multi-Reggeon system with N particles is completely solvable [13, 14]. Thus, it possesses a complete set of integrals of motion, so called conformal charges $(q_2, \bar{q}_2, q_3, \bar{q}_3, \dots, q_N, \bar{q}_N)$ that commute with the Hamiltonian. The eigenvalues of the $SL(2, \mathbb{C})$ Hamiltonian are also called the energies of the Reggeons. The Schrödinger equation for the lowest non-trivial case, *i.e.* for $N = 2$ Reggeons, was formulated and solved by Balitsky, Fadin, Kuraev and Lipatov [15, 16, 4]. They calculated the energy of the Pomeron state with $N = 2$ Reggeons. An integral equation for three and more Reggeons was formulated in Refs. [7, 8, 17] in 1980. However, it took almost twenty years to obtain the solution for $N = 3$, which corresponds also to the QCD odderon [18, 19, 20]. Finally, the solutions for higher $N = 4, \dots, 8$ have been found recently in a series of papers [21, 22, 23] written in collaboration with S.É. Derkachov, G.P. Korchemsky and A.N. Manashov. Similar approach was taken by de Vega and Lipatov [24, 25].

Description of scattering amplitudes in terms of the reggeized gluon states is most frequently used for the elastic scattering amplitude of two heavy hadrons whose masses are comparable. Here the amplitude is equal to a sum over the Regge poles. In the Regge limit, $s \rightarrow \infty$ and $t = \text{const}$ they give behaviour like $s^{\alpha(t)}$ where $\alpha(0)$ is called the intercept and its value is close to 1. On the other hand, the intercept is related to the minimum of the Reggeon energy defined by the $SL(2, \mathbb{C})$ Hamiltonian. Thus, evaluating the spectrum of the $SL(2, \mathbb{C})$ XXX Heisenberg model we can calculate the behaviour of the hadron scattering amplitudes.

Three reggeized gluon states in t -channel correspond either to Pomeron exchanges with parity $C = +1$ or to odderon states with $C = -1$. The Janik-Wosiek solutions include both of them. Using the duality symmetry as well as momentum representation Bartels, Lipatov and Vacca found another solution with $q_3 = 0$ and $\alpha(0) = 1$ [26, 27, 28, 29, 30]. On the other hand there was shown in Refs. [13, 14] that in order to solve the problem and

calculate the intercept one may use Q -Baxter method [31]. It was applied to three Reggeon problem in Refs. [21, 22, 23] and Refs. [24, 25], however only in the former ones there was a complete agreement with the Janik-Wosiek method. The intercept for the three-Reggeon function was also calculated directly using variational method in Ref. [32]. The results agree with values obtained by the exact Q -Baxter method.

In this work we present the generalized Janik-Wosiek method of constructing the Reggeon eigenstates. Moreover, we calculate the reach spectrum of the the three Reggeon energy and the spectrum of the conformal charges $\{q_3, \bar{q}_3\}$ for $n_h = 0, 1, 2, 3$. At the end we evaluate corrections to the WKB approximation [21].

In Section 2 we discuss the current state of knowledge. Next we describe construction of the Reggeon eigenfunctions that consists in solving the the differential eigenequations of the conformal charges. We systematize the knowledge about the ansatzes for eigenstates of $\{q_3, \bar{q}_3\}$ for three reggeized gluon, extend the calculations to an arbitrary complex spin s and derive differential eigenequations for the conformal charges q_3 . Moreover, we show solutions to the differential eigenequations with $N = 3$ and $s = 0$ and resum obtained series solutions for the $q_3 = 0$ case. We construct an exact solution to the \hat{q}_3 -eigenequation, which may be solved by a series method, and find the quantization conditions for $\{q_3, \bar{q}_3\}$ which come from single-valuedness of the Reggeon wave-function. The numerical results of this method for $N = 3$ are presented in Section 4. They agree with solutions found using Q -Baxter method [22, 23]. We present quantized values of q_3 for different Lorentz spins $n_h = 0, \dots, 3$ as well as corrections to the WKB approximation. At the end we make final conclusions.

2. Hamiltonian method

2.1. The formalism

In the high energy Regge limit

$$s \rightarrow \infty \quad t = \text{const} \quad (2.1)$$

the contribution to the scattering amplitude of two hadrons A and B from an exchange of three reggeized gluons may be written as

$$\mathcal{A}_{N=3}(s, t) = s \int d^2 z_0 e^{i\vec{z}_0 \cdot \vec{p}} \langle \tilde{\Phi}_A(\vec{z}_0) | e^{-\bar{\alpha}_s Y \tilde{\mathcal{H}}_3/4} \left(\tilde{\partial}_1^2 \tilde{\partial}_2^2 \tilde{\partial}_3^2 \right)^{-1} | \tilde{\Phi}_B(0) \rangle, \quad (2.2)$$

where $\partial_k = \partial/\partial z_k$, the rapidity $Y = \ln s/s_0$ and $\left(\tilde{\partial}_1^2 \tilde{\partial}_2^2 \tilde{\partial}_3^2 \right)^{-1}$ are gluon propagators. Reggeized gluon states, which are also called Reggeons, are

effective particles. They interact with each other and propagate in the t -channel. The Hamiltonian $\tilde{\mathcal{H}}_3$ is given [7, 8, 9] as a sum of $N = 3$ BFKL kernels [15, 16, 4]. The wave-functions $|\tilde{\Phi}_{A(B)}(\vec{z}_0)\rangle \equiv \tilde{\Phi}_{A(B)}(\vec{z}_i - \vec{z}_0)$ describe the coupling of three Reggeons to the scattered particles. The \vec{z}_0 -integration fixes the momentum transfer $t = -\vec{p}_T^2$ whereas the operators $1/\partial_k^2$ stand for two-dimensional transverse propagators.

Defining the functions $\tilde{\Phi}(\vec{z})$ as

$$\tilde{\Phi}(\vec{z}) = (-i)^3 \partial_{z_1} \partial_{z_2} \partial_{z_3} \Phi(\vec{z}) \quad (2.3)$$

the scalar product in the amplitude (2.2) can be rewritten as

$$\begin{aligned} \langle \tilde{\Phi}_A(\vec{z}_0) | e^{-\bar{\alpha}_s Y \tilde{\mathcal{H}}_3/4} \left(\bar{\partial}_1^2 \bar{\partial}_2^2 \bar{\partial}_3^2 \right)^{-1} | \tilde{\Phi}_B(0) \rangle &= \\ &= \langle \Phi_A(\vec{z}_0) | e^{-\bar{\alpha}_s Y \mathcal{H}_3^{(s=0, \bar{s}=1)}/4} | \Phi_B(0) \rangle. \end{aligned} \quad (2.4)$$

The Hamiltonians, \mathcal{H}_3 and $\tilde{\mathcal{H}}_3$ are invariant under the coordinate transformation of the $SL(2, \mathbb{C})$ group

$$z'_k = \frac{az_k + b}{cz_k + d}, \quad \bar{z}'_k = \frac{\bar{a}\bar{z}_k + \bar{b}}{\bar{c}\bar{z}_k + \bar{d}} \quad (2.5)$$

with $k = 1, 2, 3$ while $ad - bc = \bar{a}\bar{d} - \bar{b}\bar{c} = 1$ and they are related to each other as

$$\mathcal{H}_3^{(s=0, \bar{s}=1)} = (\bar{\partial}_1 \bar{\partial}_2 \bar{\partial}_3) \tilde{\mathcal{H}}_3 (\bar{\partial}_1 \bar{\partial}_2 \bar{\partial}_3)^{-1}. \quad (2.6)$$

Now, one may associate with each particle generators of transformation (2.5) [33]. This generators are a pair of mutually commuting holomorphic and anti-holomorphic spin operators, $S_\alpha^{(k)}$ and $\bar{S}_\alpha^{(k)}$. They satisfy the standard commutation relations $[S_\alpha^{(k)}, S_\beta^{(n)}] = i\epsilon_{\alpha\beta\gamma} \delta^{kn} S_\gamma^{(k)}$ and similarly for $\bar{S}_\alpha^{(k)}$. The generators act on the quantum space of the k -th particle, $V^{(s, \bar{s})}$ as differential operators

$$\begin{aligned} S_0^k &= z_k \partial_{z_k} + s, & S_-^{(k)} &= -\partial_{z_k}, & S_+^{(k)} &= z_k^2 \partial_{z_k} + 2sz_k, \\ \bar{S}_0^k &= \bar{z}_k \partial_{\bar{z}_k} + \bar{s}, & \bar{S}_-^{(k)} &= -\partial_{\bar{z}_k}, & \bar{S}_+^{(k)} &= \bar{z}_k^2 \partial_{\bar{z}_k} + 2\bar{s}\bar{z}_k, \end{aligned} \quad (2.7)$$

where $S_\pm^{(k)} = S_1^{(k)} \pm iS_2^{(k)}$ while the complex parameters, s and \bar{s} , are called the complex spins. Thus, the Casimir operator reads

$$\sum_{j=0}^2 (S_j^{(k)})^2 = (S_0^{(k)})^2 + (S_+^{(k)} S_-^{(k)} + S_-^{(k)} S_+^{(k)})/2 = s(s-1) \quad (2.8)$$

and similarly for the anti-holomorphic operator $(\bar{S}^{(k)})^2$. The eigenstates of the $SL(2, \mathbb{C})$ invariant system transform as [34, 35]

$$\Psi(z_k, \bar{z}_k) \rightarrow \Psi'(z_k, \bar{z}_k) = (cz_k + d)^{-2s} (\bar{c}\bar{z}_k + \bar{d})^{-2\bar{s}} \Psi(z'_k, \bar{z}'_k). \quad (2.9)$$

Due to the invariance (2.5) of the system we can rewrite the Hamiltonian as

$$\mathcal{H}_3 = H_3 + \bar{H}_3, \quad [H_3, \bar{H}_3] = 0 \quad (2.10)$$

in terms of the conformal spins (2.7)

$$H_3 = \sum_{k=1}^N H(J_{k,k+1}), \quad \bar{H}_3 = \sum_{k=1}^3 H(\bar{J}_{k,k+1}), \quad (2.11)$$

where

$$H(J) = \psi(1 - J) + \psi(J) - 2\psi(1) \quad (2.12)$$

with $\psi(x) = d \ln \Gamma(x) / dx$ being the Euler function and $J_{3,4} = J_{3,1}$. Here operators, $J_{k,k+1}$ and $\bar{J}_{k,k+1}$, are defined through the Casimir operators for the sum of the spins of the neighbouring Reggeons

$$J_{k,k+1}(J_{k,k+1} - 1) = (S^{(k)} + S^{(k+1)})^2 \quad (2.13)$$

with $S_\alpha^{(4)} = S_\alpha^{(1)}$, and $\bar{J}_{k,k+1}$ is defined similarly.

In statistical physics (2.11) is called the Hamiltonian of the non-compact $SL(2, \mathbb{C})$ XXX Heisenberg homogeneous spin magnets. It describes the nearest neighbour interaction between three non-compact $SL(2, \mathbb{C})$ spins attached to the particles with periodic boundary conditions.

In QCD values of (s, \bar{s}) depend on a chosen scalar product in the space of the wave-functions (2.9) and they are usually equal to $(0, 1)$ or $(0, 0)$ [33, 24].

In order to find the high energy behaviour of the scattering amplitude we have to solve the Schrödinger equation

$$\mathcal{H}_3^{(s=0, \bar{s}=1)} \Psi(\vec{z}_1, \vec{z}_2, \vec{z}_3) = E_N \Psi(\vec{z}_1, \vec{z}_2, \vec{z}_3) \quad (2.14)$$

with the eigenstate $\Psi(\vec{z}_1, \vec{z}_2, \vec{z}_3)$ being single-valued function on the planes $\vec{z}_k = (z_k, \bar{z}_k)$, normalizable with respect to the $SL(2, \mathbb{C})$ invariant scalar product

$$\|\Psi\|^2 = \langle \Psi | \Psi \rangle = \int d^2 z_1 d^2 z_2 d^2 z_3 |\Psi(\vec{z}_1, \vec{z}_2, \vec{z}_3)|^2, \quad (2.15)$$

where $d^2 z_i = dx_i dy_i = dz_i d\bar{z}_i / 2$ with $\bar{z}_i = z_i^*$.

From the point of view of the $SL(2, \mathbb{C})$ spin chain

$$\tilde{\mathcal{H}}_3 = \mathcal{H}_3^{(s=0, \bar{s}=0)}. \quad (2.16)$$

Indeed, the transformation $\bar{S}_\alpha \rightarrow (\bar{\partial}_1 \bar{\partial}_2 \bar{\partial}_3) \bar{S}_\alpha (\bar{\partial}_1 \bar{\partial}_2 \bar{\partial}_3)^{-1}$ maps the $\text{SL}(2, \mathbb{C})$ generators of the spin $\bar{s} = 0$ into those with the spin $\bar{s} = 1$.

One concludes from (2.15) that the Hamiltonian $\mathcal{H}_3^{(s=0, \bar{s}=1)}$ is advantageous with respect to $\tilde{\mathcal{H}}_3 = \mathcal{H}_3^{(s=0, \bar{s}=0)}$ as it has the quantum numbers of the principal series representation of the $\text{SL}(2, \mathbb{C})$ group.

However, one can also use $\mathcal{H}_3^{(s=0, \bar{s}=0)}$ [24] or even $\mathcal{H}_3^{(s=1, \bar{s}=1)}$ [25]. Then the factor $(\partial_1 \partial_2 \partial_3)^{\mp 1}$ or $(\bar{\partial}_1 \bar{\partial}_2 \bar{\partial}_3)^{\mp 1}$ has to be included in the scalar product, *i.e.* for $(s = 1, \bar{s} = 1)$ we have

$$\|\Psi\|^2 = \int d^2 z_1 d^2 z_2 d^2 z_3 |(\bar{\partial}_1 \bar{\partial}_2 \bar{\partial}_3)^{-1} \Psi(\vec{z}_1, \vec{z}_2, \vec{z}_3)|^2. \quad (2.17)$$

Here the scalar product is no longer in the principal series representation of the $\text{SL}(2, \mathbb{C})$ group. All these Hamiltonians with the corresponding scalar products are equivalent up to the zero modes of the operators $(\partial_1 \partial_2 \partial_3)^{\mp 1}$ and $(\bar{\partial}_1 \bar{\partial}_2 \bar{\partial}_3)^{\mp 1}$.

A part of the amplitude (2.2) for $N = 3$ reggeized gluons describes the leading contribution of the states with parity $C = -1$, odderon, and subleading contribution to the $C = +1$ states related to the Pomeron. Both contributions are of the same order.

Instead solving the Hamiltonian eigenproblem (2.14) we can solve eigenproblems for conformal charges

$$\begin{aligned} \hat{q}_2 &= -2 \sum_{i_2 > i_1 = 1}^N \left(\sum_{j_1=0}^2 S_{j_1}^{(i_1)} S_{j_1}^{(i_2)} \right) \\ &= \sum_{i_2 > i_1 = 1}^N \left((z_{i_2 i_1})^{2(1-s)} \partial_{z_{i_2}} \partial_{z_{i_1}} (z_{i_2 i_1})^{2s} + 2s(s-1) \right), \\ \hat{q}_3 &= 2 \sum_{i_1, i_2, i_3=1}^N \varepsilon_{i_1 i_2 i_3} S_0^{(i_1)} S_1^{(i_2)} S_2^{(i_3)} \\ &= i^3 \sum_{i_3 > i_2 > i_1 = 1}^N \left(z_{i_1 i_2} z_{i_2 i_3} z_{i_3 i_1} \partial_{z_{i_3}} \partial_{z_{i_2}} \partial_{z_{i_1}} + s z_{i_1 i_2} (z_{i_2 i_3} - z_{i_3 i_1}) \partial_{z_{i_2}} \partial_{z_{i_1}} \right. \\ &\quad \left. + s z_{i_2 i_3} (z_{i_3 i_1} - z_{i_1 i_2}) \partial_{z_{i_3}} \partial_{z_{i_2}} + s z_{i_3 i_1} (z_{i_3 i_1} - z_{i_1 i_2}) \partial_{z_{i_3}} \partial_{z_{i_2}} \right. \\ &\quad \left. - 2s^2 z_{i_1 i_2} \partial_{z_{i_3}} - 2s^2 z_{i_2 i_3} \partial_{z_{i_1}} - 2s^2 z_{i_3 i_1} \partial_{z_{i_2}} \right), \end{aligned} \quad (2.18)$$

where $z_{ij} = z_i - z_j$. Similar relations hold for the anti-holomorphic sector. This gives for the $\text{SL}(2, \mathbb{C})$ spin $s = 0$

$$\hat{q}_3 = -i z_{12} z_{23} z_{31} \partial_{z_1} \partial_{z_2} \partial_{z_3} \quad (2.19)$$

and for $s = 1$

$$\hat{q}_3 = -i\partial_{z_1}\partial_{z_2}\partial_{z_3}z_{12}z_{23}z_{31}. \quad (2.20)$$

The eigenvalues of the quadratic conformal charge read:

$$q_2 = -h(h-1) + 3s(s-1) \quad \bar{q}_2 = -\bar{h}(\bar{h}-1) + 3\bar{s}(\bar{s}-1) \quad (2.21)$$

where conformal weights satisfy

$$h = \frac{1+n_h}{2} + i\nu_h, \quad \bar{h} = \frac{1-n_h}{2} + i\nu_h, \quad (2.22)$$

while the eigenvalues of the cubic operator $\bar{q}_3 = q_3^*$. The parameter n_h has the meaning of the two-dimensional Lorentz spin of the particle, whereas ν_h defines its scaling dimension. They define the transformation law of the Hamiltonian eigenstates

$$\begin{aligned} \Psi(\vec{z}'_{10'}, \vec{z}'_{20'}, \vec{z}'_{30'}) &= (cz_0 + d)^{2h}(\bar{c}\bar{z}_0 + \bar{d})^{2\bar{h}} \\ &\times \left(\prod_{k=1}^3 (cz_k + d)^{2s_k}(\bar{c}\bar{z}_k + \bar{d})^{2\bar{s}_k} \right) \Psi(\vec{z}_{10}, \vec{z}_{20}, \vec{z}_{30}) \end{aligned} \quad (2.23)$$

with

$$\Psi_{\vec{p}}(\vec{z}_1, \vec{z}_2, \vec{z}_3) = \int d^2z_0 e^{i\vec{z}_0 \cdot \vec{p}} \Psi(\vec{z}_1 - \vec{z}_0, \vec{z}_2 - \vec{z}_0, \vec{z}_3 - \vec{z}_0). \quad (2.24)$$

The eigenstates $\Psi(\vec{z}_{10}, \vec{z}_{20}, \vec{z}_{30})$ belonging to $V^{(h, \bar{h})}$ are labelled by the centre-of-mass coordinate \vec{z}_0 and can be chosen to have the $SL(2, \mathbb{C})$ transformation properties with z_0 and \bar{z}_0 transforming in the same way as z_k and \bar{z}_k , (2.5).

Conformal charges commute also with cyclic particle permutation operator

$$\mathbb{P}\Psi_{q, \bar{q}}(\vec{z}_1, \vec{z}_2, \vec{z}_3) \stackrel{\text{def}}{=} \Psi_{q, \bar{q}}(\vec{z}_2, \vec{z}_3, \vec{z}_1) = e^{i\theta_3(q, \bar{q})} \Psi_{q, \bar{q}}(\vec{z}_1, \vec{z}_2, \vec{z}_3), \quad (2.25)$$

where the conformal charges are denoted by $q \equiv (q_2, q_3)$ and $\bar{q} \equiv (\bar{q}_2, \bar{q}_3)$.

The phase $\theta_3(q)$ which is connected with eigenvalues of \mathbb{P} is called the quasimomentum. It takes the following values [21]

$$\theta_3(q, \bar{q}) = 2\pi \frac{k}{3}, \quad \text{for } k = 0, 1, \dots, 2. \quad (2.26)$$

The eigenstates of the conformal charges \hat{q}_k diagonalize \mathcal{H} and \mathbb{P} .

Let us also define another operator

$$\mathbb{M}\Psi^\pm(\vec{z}_1, \vec{z}_2, \vec{z}_3) \stackrel{\text{def}}{=} \Psi^\pm(\vec{z}_3, \vec{z}_2, \vec{z}_1) = \pm\Psi^\pm(\vec{z}_1, \vec{z}_2, \vec{z}_3), \quad (2.27)$$

so called mirror permutation operator which has two eigenvalues, ± 1 . The \mathbb{M} operator commutes with the Hamiltonian but it does not commute with \hat{q}_2 and \bar{q}_3 .

The cyclic and mirror permutation symmetries come from the Bose symmetry. Physical states should possess both symmetries.

It turns out that adding colour factor corresponding to the antisymmetric constant f_{abc} for the odd-mirror states and the symmetric one d_{abc} for the even-mirror states, we are able to restore Bose symmetry. The tensor f_{abc} corresponds to the Pomeron states while d_{abc} is related to the odderon states. Therefore, in order to check a C -parity of a given state we need to study its parity under the mirror permutation \mathbb{M} . The states Ψ satisfying $\mathbb{M}\Psi = -\Psi$ are the Pomeron states whereas states for which $\mathbb{M}\Psi = +\Psi$ are the odderon states.

3. Various ansatzes

Using the eigenequation for \hat{q}_2 we get Lipatov's ansatz [26] for holomorphic part of the eigenstates:

$$\Psi(z_{10}, z_{20}, z_{30}) = \frac{1}{(z_{10}z_{20}z_{30})^{2s}} \left(\frac{z_{31}}{z_{10}z_{30}} \right)^{h-3s} F(x), \quad (3.1)$$

where $x = \frac{z_{12}z_{30}}{z_{10}z_{32}}$. If we substitute $F(x) = G(x) \left(\frac{(x-1)^2}{-x} \right)^{h/3-s}$ we get another ansatz

$$\Psi(z_{10}, z_{20}, z_{30}) = \frac{1}{(z_{12}z_{23}z_{31})^s} \left(\frac{z_{31}z_{12}z_{23}}{(z_{10})^2(z_{20})^2(z_{30})^2} \right)^{\frac{h}{3}} G(x). \quad (3.2)$$

As we can see we obtained a totally symmetric ansatz which is equivalent to the original one.

Both ansatzes have advantages and disadvantages. The symmetric one (3.2) is appropriate if we want to deal with the particle symmetries. The original one (3.1) has a simpler structure, it contains powers of h (not $h/3$), so we can use it when we want to construct proper single-valuedness conditions. One can easily notice that $z^{\frac{h}{3}} \bar{z}^{\bar{h}}$ is single-valued because $h - \bar{h} = n_h \in \mathbb{Z}$.

3.1. Derivation of differential equations for $N = 3$

From the \hat{q}_3 -eigenequation we get the third order differential equation

$$\begin{aligned} iq_3 F(x) &= (3s - h)(h - 1 - s)(1 - 2x)F(x) + (((h - 2)(h - 1)(x - 1)x \\ &+ s^2(2 + 11(x - 1)x) + s(2 - 2h(1 - 2x)^2 + 11(x - 1)x))F'(x) \\ &+ (2 + h - 3s)(1 - x)x(2x - 1)F''(x) + (x - 1)^2 x^2 F^{(3)}(x), \end{aligned} \quad (3.3)$$

where q_3 is a complex eigenvalue of \hat{q}_3 . From the QCD point of view the most interesting cases are for $s = 0$:

$$\begin{aligned} iq_3 F(x) &= (h - 1)(h - 2)x(x - 1)F'(x) \\ &+ (h - 2)(x - 1)x(1 - 2x)F''(x) + x^2(x - 1)^2 F^{(3)}(x) \end{aligned} \quad (3.4)$$

and for $s = 1$

$$\begin{aligned} iq_3 F(x) &= (h - 3)(h - 2)(2x - 1)F(x) + \\ &+ ((4 - 2h - (h - 8)(h - 3)x + (h - 8)(h - 3)x^2)F'(x) \\ &+ (5 - h)(x - 1)x(2x - 1)F''(x) + (x - 1)^2 x^2 F^{(3)}(x). \end{aligned} \quad (3.5)$$

The first such solution was derived and found numerically in [18].

We solve the above equations by the series method choosing representation $(s, \bar{s}) = (0, 0)$ which gives the same equation in holomorphic and antiholomorphic sectors. The differential equation (3.4) has three regular singular points at $x = 0$, $x = 1$ and $x = \infty$. To generate solutions around other singular points we exchange variables. For the case $x = 1$ we can use a substitution $x = 1 - y$:

$$\begin{aligned} iq_3 G(y) &= (h - 1)(h - 2)y(1 - y)G'(y) \\ &+ (h - 2)(1 - y)y(1 - 2y)G''(y) - y^2(y - 1)^2 G^{(3)}(y). \end{aligned} \quad (3.6)$$

with $F(1 - y) = G(y)$ and for $x = \infty$ we have $x = 1/y$:

$$\begin{aligned} q_3 G(y) &= i((y - 1)(h + 1)(h - 2y)G'(y) \\ &+ (y - 1)y(2(h + 1) - (h + 4)y)G''(y) + y(y - 1)^2 G^{(3)}(y)). \end{aligned} \quad (3.7)$$

where $F(1/y) = G(y)$.

In Ref. [18] Eq. (3.4) was solved for the case with $h = \bar{h} = 1/2$ and $\text{Re}[q_3] = 0$. Next in Refs. [36, 37, 38] states with $n_h = 0, 2$ and $\nu_h \in \mathbb{R}$ as well as $n_h = 0$ and $i\nu_h \in \mathbb{R}$ were found. In this work we extend these calculations to $n_h = 0, 1, 2, 3$ and $\nu_h \in \mathbb{R}$. To get a broader perspective on the problem the reader is referred to Ref. [39].

3.2. Wave-function for $s = \bar{s} = 0$ around $x = \bar{x} = 0$

In order to obtain the full-complex solution for three-Reggeon state containing the holomorphic and anti-holomorphic parts we have to glue together solutions in these sectors:

$$\Phi_{q,\bar{q}}(\{z_i\}, \{\bar{z}_i\}) = \bar{u}_{\bar{q}}(\{\bar{z}_i\})^T \cdot A^{(0)}(h, \bar{h}, q_3, \bar{q}_3) \cdot u_q(\{z_i\}), \quad (3.8)$$

where we use a (3×3) mixing-matrix, $A_{q,\bar{q}}^{(0)}$, [18] which does not depend on particle coordinates but only on $q \equiv \{q_2, q_3\}$. From the QCD point of view we have two possibilities of gluing solutions: $(s = 0, \bar{s} = 0)$ [24] and $(s = 0, \bar{s} = 1)$ [33]. These two cases are equivalent except for the zero modes of the highest conformal charge \hat{q}_N . Let us consider the first case, $s = \bar{s} = 0$.

The antiholomorphic and holomorphic conformal charges are related by conditions $\bar{h} = 1 - h^*$ and $\bar{q}_k = q_k^*$. The wave-function has to be single-valued. This condition defines the structure of the mixing-matrix.

For $h \notin \mathbb{Z}$ and $\hat{q}_3 \neq 0$ we have solutions of the following type

$$\begin{aligned} u_1(x) &= x^h \sum_{n=0}^{\infty} a_{n,r_1} x^n, \\ u_2(x) &= x^1 \sum_{n=0}^{\infty} a_{n,r_2} x^n, \\ u_3(x) &= x^0 \sum_{n=0}^{\infty} b_{n,r_3} x^n + x^1 \sum_{n=0}^{\infty} a_{n,r_2} x^n \text{Log}(x) \end{aligned} \quad (3.9)$$

and similarly in the anti-holomorphic sector. The recurrence relations for the a_{n,r_i} are given in Appendix C. One can notice that $x^a \bar{x}^b$ is single-valued only if $a - b \in \mathbb{Z}$. Moreover we have also terms with $\text{Log}(x)$ which have to give in a sum $\text{Log}(x\bar{x})$. So in this case we have a mixing matrix of the form

$$A^{(0)}(h, \bar{h}, q_3, \bar{q}_3) = \begin{bmatrix} \alpha & 0 & 0 \\ 0 & \beta & \gamma \\ 0 & \gamma & 0 \end{bmatrix}, \quad (3.10)$$

where α, β, γ are arbitrary. In the above matrix we have $A_{12} = A_{13} = A_{21} = A_{31} = 0$ in order to eliminate multi-valuedness coming from the power-terms, $A_{23} = A_{32}$ to obtain single-valuedness in $\text{Log}(x)$ -terms and $A_{33} = 0$ because the term $\text{Log}(x)\text{Log}(\bar{x})$ is not single-valued on the \vec{x} -plane.

In the case of $q_3 = 0$ and $h \notin \{0, 1\}$ we don't have any $\text{Log}(x)$ -terms so

the mixing matrix looks like ¹

$$A^{(0)}(h, \bar{h}, q_3 = 0, \bar{q}_3 = 0) = \begin{bmatrix} \beta & 0 & 0 \\ 0 & \alpha & \rho \\ 0 & \varepsilon & \gamma \end{bmatrix}. \quad (3.11)$$

For $q_3 \neq 0$ and $h \in \mathbb{Z}$ we have a solution with only integer powers of x and solutions without a Log, with one-Log and with a double-Log. The structure of the matrix is

$$A^{(0)}(h \in \mathbb{Z}, \bar{h} \in \mathbb{Z}, q_3, \bar{q}_3) = \begin{bmatrix} \alpha & \beta & \gamma \\ \beta & 2\gamma & 0 \\ \gamma & 0 & 0 \end{bmatrix}. \quad (3.12)$$

In the last case for $q_3 = 0$ and $h \in \{0, 1\}$ we have only integer powers of x and the third solution with one-Log term. The matrix has a form

$$A^{(0)}(h \in \{0, 1\}, \bar{h} \in \{0, 1\}, q_3 = 0, \bar{q}_3 = 0) = \begin{bmatrix} \alpha & \gamma & 0 \\ \beta & \rho & \varepsilon \\ 0 & \varepsilon & 0 \end{bmatrix}. \quad (3.13)$$

3.3. Wave-function for $s = \bar{s} = 0$ around $x = \bar{x} = 1^-$ and $x = \bar{x} = \infty^-$

We construct the wave-function around the other singular point exactly in the same way, obtaining matrices $A^{(1^-)}(h, \bar{h}, q_3, \bar{q}_3)$, $A^{(1^+)}(h, \bar{h}, q_3, \bar{q}_3)$ (around 1) and $A^{(\infty^-)}(h, \bar{h}, q_3, \bar{q}_3)$ (around ∞).

Thus, we have the wave-functions similar to (3.8). For $h \notin \mathbb{Z}$ and $\hat{q}_3 \neq 0$ get

$$\begin{aligned} u_1(x) &= (1-x)^h \sum_{n=0}^{\infty} a_{n,r_1} (1-x)^n, \\ u_2(x) &= (1-x)^1 \sum_{n=0}^{\infty} a_{n,r_2} (1-x)^n, \\ u_3(x) &= (1-x)^0 \sum_{n=0}^{\infty} b_{n,r_3} (1-x)^n + (1-x)^1 \sum_{n=0}^{\infty} a_{n,r_2} (1-x)^n \text{Log}(1-x) \end{aligned} \quad (3.14)$$

and similarly in the anti-holomorphic sector. The mixing matrices take the following forms

$$A^{(1)}(h, \bar{h}, q_3, \bar{q}_3) = \begin{bmatrix} \alpha & 0 & 0 \\ 0 & \beta & \gamma \\ 0 & \gamma & 0 \end{bmatrix}, \quad (3.15)$$

¹ Greek variables in each A -matrix have different numerical values

$$A^{(1)}(h, \bar{h}, q_3 = 0, \bar{q}_3 = 0) = \begin{bmatrix} \beta & 0 & 0 \\ 0 & \alpha & \rho \\ 0 & \varepsilon & \gamma \end{bmatrix}, \quad (3.16)$$

$$A^{(1)}(h \in \mathbb{Z}, \bar{h} \in \mathbb{Z}, q_3, \bar{q}_3) = \begin{bmatrix} \alpha & \beta & \gamma \\ \beta & 2\gamma & 0 \\ \gamma & 0 & 0 \end{bmatrix}, \quad (3.17)$$

$$A^{(1)}(h \in \{0, 1\}, \bar{h} \in \{0, 1\}, q_3 = 0, \bar{q}_3 = 0) = \begin{bmatrix} \alpha & \gamma & 0 \\ \beta & \rho & \varepsilon \\ 0 & \varepsilon & 0 \end{bmatrix}. \quad (3.18)$$

Similarly, we proceed around $x = \infty^-$. For $h \notin \mathbb{Z}$ and $\hat{q}_3 \neq 0$ we have solutions of type

$$u_1(x) = (1/x)^0 \sum_{n=0}^{\infty} a_{n,r_1} (1/x)^n, \quad (3.19)$$

$$u_2(x) = (1/x)^{1-h} \sum_{n=0}^{\infty} a_{n,r_2} (1/x)^n,$$

$$u_3(x) = (1/x)^{-h} \sum_{n=0}^{\infty} b_{n,r_3} x^n + (1/x)^{1-h} \sum_{n=0}^{\infty} a_{n,r_2} x^n \text{Log}(x)$$

and similarly in the anti-holomorphic region. In this case we have the matrices

$$A^{(\infty)}(h, \bar{h}, q_3, \bar{q}_3) = \begin{bmatrix} \alpha & 0 & 0 \\ 0 & \beta & \gamma \\ 0 & \gamma & 0 \end{bmatrix}, \quad (3.20)$$

$$A^{(\infty)}(h, \bar{h}, q_3 = 0, \bar{q}_3 = 0) = \begin{bmatrix} \beta & 0 & 0 \\ 0 & \alpha & \rho \\ 0 & \varepsilon & \gamma \end{bmatrix}, \quad (3.21)$$

$$A^{(\infty)}(h \in \mathbb{Z}, \bar{h} \in \mathbb{Z}, q_3, \bar{q}_3) = \begin{bmatrix} \alpha & \beta & \gamma \\ \beta & 2\gamma & 0 \\ \gamma & 0 & 0 \end{bmatrix}, \quad (3.22)$$

$$A^{(\infty)}(h \in \{0, 1\}, \bar{h} \in \{0, 1\}, q_3 = 0, \bar{q}_3 = 0) = \begin{bmatrix} \alpha & \gamma & 0 \\ \beta & \rho & \varepsilon \\ 0 & \varepsilon & 0 \end{bmatrix}. \quad (3.23)$$

3.4. Transition matrices between solutions around different poles

The above solutions around $x = 0, 1, \infty$ have a convergence radius equal to the difference between the two singular points: the point around which the solution is defined and the nearest one of the remaining two. In order to define a global solution which is convergent in the entire complex plane we have to glue the solutions defined around different singular points. This can be done by expanding one set of solutions in terms of the other solutions in the overlap region of the two considered solutions. Thus, in the overlap region we can define the transition matrices Δ, Γ , where

$$\begin{aligned}\bar{u}^{(0)}(x, q) &= \Delta(q)\bar{u}^{(1)}(x, q), \\ \bar{u}^{(1)}(x, q) &= \Gamma(q)\bar{u}^{(\infty)}(x, q).\end{aligned}\tag{3.24}$$

Matrices, Δ and Γ , are constructed in terms of the ratios of certain determinants [40]. For example, to calculate the matrix Δ we construct a Wronskian

$$W = \begin{vmatrix} u_1^{(1)}(x; q) & u_2^{(1)}(x; q) & u_3^{(1)}(x; q) \\ u_1^{\prime(1)}(x; q) & u_2^{\prime(1)}(x; q) & u_3^{\prime(1)}(x; q) \\ u_1^{\prime\prime(1)}(x; q) & u_2^{\prime\prime(1)}(x; q) & u_3^{\prime\prime(1)}(x; q) \end{vmatrix}.\tag{3.25}$$

Next we construct determinants W_{ij} which are obtained from W by replacing j -th column by the i -th solution around $x = 0$, *i.e.* for $i = 1$ and $j = 2$ we have

$$W_{12} = \begin{vmatrix} u_1^{(1)}(x; q_3) & u_1^{(0)}(x; q_3) & u_3^{(1)}(x; q_3) \\ u_1^{\prime(1)}(x; q_3) & u_1^{\prime(0)}(x; q_3) & u_3^{\prime(1)}(x; q_3) \\ u_1^{\prime\prime(1)}(x; q_3) & u_1^{\prime\prime(0)}(x; q_3) & u_3^{\prime\prime(1)}(x; q_3) \end{vmatrix}.\tag{3.26}$$

The matrix elements Δ_{ij} are given by

$$\Delta_{ij} = \frac{W_{ij}}{W}.\tag{3.27}$$

Matrix Δ does not depend on x , but only on q_k . In the similar way we can get matrices Γ and their anti-holomorphic equivalents: $\bar{\Delta}, \bar{\Gamma}$.

Substituting equation (3.24) into the wave-function (3.8), one finds the following conditions for continuity of the matrix $A(\bar{q}, q)$:

$$\bar{\Delta}^T(\bar{q}_3)A^{(0)}(\bar{q}_3, q_3)\Delta(q_3) = A^{(1)}(\bar{q}_3, q_3),\tag{3.28}$$

$$\bar{\Gamma}^T(\bar{q}_3)A^{(1)}(\bar{q}_3, q_3)\Gamma(q_3) = A^{(\infty)}(\bar{q}_3, q_3).\tag{3.29}$$

Each Equation, (3.28)-(3.29), consists of nine equations. Solving them numerically, we obtain values of parameters $\alpha, \beta, \gamma, \dots$ as well as quantized

values of the conformal charges, q_k and \bar{q}_k . We have verified numerically that the spectrum of q_k obtained by the above method is equivalent to the spectrum obtained using the Baxter Q -operator method which is presented in next Section.

3.5. Additional conditions coming from the particle permutation invariance

Multi-Reggeon states have additionally the cyclic (2.25) and mirror permutation (2.27) symmetries. The conformal charges commute only with \mathbb{P} . Thus, the eigenstates of \hat{q}_2 and \hat{q}_3 (2.18) are usually not eigenstates of \mathbb{M} , so they usually have mixed C -parity. Therefore in order to get solutions of a given C -parity we have to impose mirror symmetry. Let us illustrate this for the case of $q_3 = 0$.

For this case we can easily resum the series solutions, see Appendix C. Let us take the case for $h \notin \{0, 1\}$. The eigenequation for the cyclic permutation \mathbb{P} with quasimomentum $\theta_3(q)$ gives the following condition

$$\begin{aligned} w^h \bar{w}^{\bar{h}} & \left(\beta + \gamma(-x)^h (-\bar{x})^{\bar{h}} + \alpha(x-1)^h (\bar{x}-1)^{\bar{h}} \right. \\ & \left. + \rho(-x)^h (\bar{x}-1)^{\bar{x}} + \varepsilon(x-1)^h (-\bar{x})^{\bar{h}} \right) = \\ & = e^{i\theta_3(q)} w^h \bar{w}^{\bar{h}} \left(\alpha + \beta(-x)^h (-\bar{x})^{\bar{h}} + \gamma(x-1)^h (\bar{x}-1)^{\bar{h}} \right. \\ & \left. + \rho(x-1)^h + \varepsilon(\bar{x}-1)^{\bar{h}} \right). \end{aligned} \quad (3.30)$$

Here we have used cyclic transformation laws (A.6).

Comparing these two lines we obtain conditions: $\alpha = e^{-i\theta_3(q)}\beta$, $\beta = e^{-i\theta_3(q)}\gamma$, $\gamma = e^{-i\theta_3(q)}\alpha$ and $\rho = \varepsilon = 0$. One can derive that $\exp(3i\theta_3(q)) = 1$ so $\theta_3(q) = \frac{2k\pi}{3}$ where $k = 0, 1, 2$ ($k = 0$ for physical states). Thus the eigenstate of \mathbb{P} [27] reads

$$\begin{aligned} \Psi(\vec{z}_{10}, \vec{z}_{20}, \vec{z}_{30}) & = \\ & = w^h \bar{w}^{\bar{h}} \left(1 + e^{i\frac{2\pi k}{3}} (-x)^h (-\bar{x})^{\bar{h}} + e^{i\frac{4\pi k}{3}} (x-1)^h (\bar{x}-1)^{\bar{h}} \right), \end{aligned} \quad (3.31)$$

with $k = 0, 1, 2$ and where we have omitted the normalization constant.

Now we can act with a mirror permutation operator on (2.25) and test its eigenequation (2.27). Using the mirror transformations (A.7), similarly to (3.30), we obtain the following relation

$$\begin{aligned} w^h \bar{w}^{\bar{h}} (-1)^{n_h} & \left(e^{i\frac{2\pi k}{3}} + (-x)^h (-\bar{x})^{\bar{h}} + e^{i\frac{4\pi k}{3}} (x-1)^h (\bar{x}-1)^{\bar{h}} \right) = \\ & = \pm w^h \bar{w}^{\bar{h}} \left(1 + e^{i\frac{2\pi k}{3}} (-x)^h (-\bar{x})^{\bar{h}} + e^{i\frac{4\pi k}{3}} (x-1)^h (\bar{x}-1)^{\bar{h}} \right). \end{aligned} \quad (3.32)$$

Comparing both sides of (3.32) gives $(-1)^{n_h} \exp(i\frac{2\pi k}{3}) = \pm 1$, $(-1)^{n_h} = \pm \exp(i\frac{2\pi k}{3})$ and $(-1)^{n_h} = \pm 1$ where the $SL(2, \mathbb{C})$ Lorentz spins $n_h = h - \bar{h}$. These conditions are consistent with $k = 0, \frac{3}{2}$. Only the first case agrees with the cyclic permutation condition. As we can see for odd n_h we have *minus* sign, so taking into account colour factors $(-1)^N$, solution (3.32) is C -even. For even n_h we have *plus* sign thus solution is C -odd. The last case is unnormalizable because when $x \rightarrow 0$ or $x \rightarrow 1$ it does not vanish so the norm, with $(s = 0, \bar{s} = 0)$, is divergent [27].

Using the duality symmetry [26, 27, 28, 29, 30], which corresponds to $h \rightarrow 1 - h$, Bartels, Lipatov and Vacca constructed an eigenstate with $q_3 = 0$ and $C = -1$

$$\begin{aligned} \Psi(\vec{z}_{10}, \vec{z}_{20}, \vec{z}_{30}) &= \\ &= w^h \bar{w}^{\bar{h}} x(1-x) \bar{x}(1-\bar{x}) \left(\delta^{(2)}(x) - \delta^{(2)}(1-x) + \frac{x^h \bar{x}^{\bar{h}}}{x^3 \bar{x}^3} \delta^{(2)}\left(\frac{1}{x}\right) \right). \end{aligned} \quad (3.33)$$

This wave-function cannot be constructed using the method described here because it contains non-analytical function, the Dirac delta $\delta^{(2)}(x)$.

Now, let us take the second wave-function with five parameters *i.e.* for $q_3 = 0$ and $h \in \{0, 1\}$. For $h = 1$ the vector of linearly independent solutions reads

$$u(x) = [1, (-x), (-x)\text{Log}(-x) + (x-1)\text{Log}(x-1)] \quad (3.34)$$

and for $\bar{h} = 0$ it is

$$\bar{u}(\bar{x}) = [\text{Log}(\bar{x}-1), 1, \text{Log}(-\bar{x})]. \quad (3.35)$$

Combining them we obtain

$$\begin{aligned} \Psi(\vec{z}_{10}, \vec{z}_{20}, \vec{z}_{30}) &= w^h \bar{w}^{\bar{h}} (\alpha \text{Log}(\bar{x}-1) + \beta + \gamma(-x)\text{Log}(\bar{x}-1) + \rho(-x) \\ &\quad + \varepsilon((-x)\text{Log}(-\bar{x}) + (-x)\text{Log}(-x) + (x-1)\text{Log}(x-1))). \end{aligned} \quad (3.36)$$

Like in the previous case we write the eigenequation for the cyclic permutation

$$\begin{aligned} w^{h(=1)} \bar{w}^{\bar{h}(=0)} &((\alpha - \gamma - \varepsilon)\text{Log}(x-1) + (\rho - \beta) + \alpha(-x)\text{Log}(\bar{x}-1) \\ &\quad + (-\beta)(-x) + \varepsilon(-x)\text{Log}(-x) + \alpha(x-1)\text{Log}(-\bar{x}) \\ &\quad + \varepsilon(-x)\text{Log}(-x) + \gamma\text{Log}(-\bar{x}) + \varepsilon(x-1)\text{Log}(x-1)) = \\ &= e^{i\theta_3(q)} w (\alpha \text{Log}(\bar{x}-1) + \beta + \gamma(-x)\text{Log}(\bar{x}-1) + \rho(-x) \\ &\quad + \varepsilon((-x)\text{Log}(-\bar{x}) + (-x)\text{Log}(-x) + (x-1)\text{Log}(x-1))). \end{aligned} \quad (3.37)$$

Thus we get conditions: $\alpha = e^{-i\theta_3(q)}(\alpha - \gamma - \varepsilon)$, $\beta = e^{-i\theta_3(q)}(\rho - \beta)$, $\gamma = e^{-i\theta_3(q)}\alpha$, $\rho = e^{-i\theta_3(q)}(-\beta)$, $0 = e^{-i\theta_3(q)}(\gamma - \alpha)$ and $\varepsilon = e^{-i\theta_3(q)}\varepsilon$. We have two types of solutions.

The first one with $\theta_3(q) = 0$ when $\alpha = \gamma = -\varepsilon$ and $\beta = \rho = 0$. It has a form

$$\Psi(\vec{z}_{10}, \vec{z}_{20}, \vec{z}_{30}) = w((-x)\text{Log}((-\bar{x})(-x)) + (x-1)\text{Log}((\bar{x}-1)(x-1))) . \quad (3.38)$$

We obtained in this way solutions with $\text{Log}(x)$ -terms which have not been found before. The similar expressions were shown in [24] as asymptotics of the \hat{q}_3 eigenfunction. Acting with the mirror permutation operator on (3.38) we get

$$\begin{aligned} \mathbb{M}w((-x)\text{Log}((-\bar{x})(-x)) + (x-1)\text{Log}((\bar{x}-1)(x-1))) = \\ = -w((-x)\text{Log}((-\bar{x})(-x)) + (x-1)\text{Log}((\bar{x}-1)(x-1))) . \end{aligned} \quad (3.39)$$

We obtained *minus* sign so this state is also symmetric under C -parity (*i.e.* with $C = +1$).

Other solutions have $\theta_3(q) = 2\pi/3, 4\pi/3$. Thus, $\alpha = \gamma = \varepsilon = 0$ and $\rho = -e^{-i\theta_3(q)}\beta$. The wave-function has a form

$$\Psi(\vec{z}_{10}, \vec{z}_{20}, \vec{z}_{30}) = w(1 + x e^{i\theta_3(q)}) . \quad (3.40)$$

These solutions are not eigenstates of the \mathbb{M} operator.

4. Known features of the spectrum

In this Section we describe the spectra of the conformal charges obtained by numerical solutions [23, 38]. To this end we apply the Baxter operator method and the Janik-Wosiek method described in the previous Section. For $N = 3$ reggeized gluons the Hamiltonian method and the Baxter operator method give the same results.

4.1. Advantages of Q -Baxter operator method

In order to find the spectrum of the conformal charges for higher N and the Reggeon energy E_N one can use the Q -Baxter operator method [31, 23]. The Baxter operator $\mathbb{Q}(u, \bar{u})$ depends on two complex spectral parameters u, \bar{u} and commutes with the integrals of motion, q_k and \bar{q}_k . It satisfies the Baxter equation:

$$\hat{t}_N(u)\mathbb{Q}(u, \bar{u}) = (u + is)^N \mathbb{Q}(u + i, \bar{u}) + (u - is)^N \mathbb{Q}(u - i, \bar{u}) , \quad (4.1)$$

$$\hat{t}_N(\bar{u})\mathbb{Q}(u, \bar{u}) = (\bar{u} + i\bar{s})^N \mathbb{Q}(u, \bar{u} + i) + (\bar{u} - i\bar{s})^N \mathbb{Q}(u, \bar{u} - i) , \quad (4.2)$$

where $\hat{t}_N(u)$ is the auxiliary transfer matrix

$$\hat{t}_N(u) = 2u^N + \hat{q}_2 u^{N-2} + \dots + \hat{q}_N \quad (4.3)$$

and similarly $\hat{t}_N(\bar{u})$. We solve the Baxter equations [23] using the integral ansatz which changes Equations 4.1 and 4.2 to differential equations. The latter ones can be solved analogically to the Janik-Wosiek method which gives Q -Baxter quantization conditions.

The Reggeon energy is determined by eigenvalues of the Baxter operator, $Q_{q_k, \bar{q}_k}(u, \bar{u})$ and can be written as

$$E_N(q, \bar{q}) = -\text{Im} \frac{d}{du} \ln \left[u^{2N} Q_{q, \bar{q}}(u + i(1-s), u + i(1-\bar{s})) \times Q_{-q, -\bar{q}}(u + i(1-s), u + i(1-\bar{s})) \right] \Big|_{u=0}, \quad (4.4)$$

with

$$\pm q = (q_2, \pm q_3, \dots, (\pm)^N q_N) \quad (4.5)$$

while the quasimomentum θ_N

$$\theta_N = i \ln \frac{Q_{q, \bar{q}}(is, i\bar{s})}{Q_{q, \bar{q}}(-is, -i\bar{s})}. \quad (4.6)$$

4.2. Trajectories

Solving the Q -Baxter quantization conditions [23] we obtain continuous trajectories in the space of conformal charges. They are built of points, $(q_2(\nu_h), \dots, q_N(\nu_h))$ which depend on a continuous real parameter ν_h entering q_2 , (2.21) and (2.22). In order to label the trajectories we introduce the set of the integers

$$\boldsymbol{\ell} = \{\ell_1, \ell_2, \dots, \ell_{2(N-2)}\} \quad (4.7)$$

which parameterize one specified point on each trajectory for given h . Specific examples in the following sections will further clarify this point.

Next we calculate the observables along these trajectories, namely the energy (2.14) and the quasimomentum (2.26). The quasimomentum is constant for all points situated on a given trajectory. The minimum of the energy, which means the maximal intercept, for almost all trajectories is located at $\nu_h = 0$. It turns out that the energy behaves around $\nu_h = 0$ like

$$E_N(\nu_h; \boldsymbol{\ell}^{\text{ground}}) = E_N^{\text{ground}} + \sigma_N \nu_h^2 + \mathcal{O}(\nu_h^2) \quad (4.8)$$

Thus, the ground state along its trajectory is gapless and the leading contribution to the scattering amplitude around ν_h may be rewritten as a series in the strong coupling constant:

$$\mathcal{A}(s, t) \sim -is \sum_{N=2}^{\infty} (i\bar{\alpha}_s)^N \frac{s^{-\bar{\alpha}_s E_N^{\text{ground}}/4}}{(\bar{\alpha}_s \sigma_N \ln s)^{1/2}} \xi_{A,N}(t) \xi_{B,N}(t), \quad (4.9)$$

where $\bar{\alpha}_s = \alpha_s N_c / \pi$ and $\xi_{X,N}(t)$ are the impact factors corresponding to the overlap between the wave-functions of scattered particle with the wave-function of N -Reggeons, whereas σ_N measures the dispersion of the energy on the the trajectory around $\nu_h = 0$.

On the other hand, the energy along the trajectories grows with ν_h and for $|\nu_h| \rightarrow \infty$ and finally, we have $E_N(\nu_h; \ell) \sim \ln \nu_h^2$. These parts of the trajectory give the lowest contribution to the scattering amplitude.

4.3. Symmetries

The spectrum of quantized charges q_2, \dots, q_N is degenerate. This degeneration is caused by two symmetries:

$$q_k \leftrightarrow (-1)^k q_k \quad (4.10)$$

which comes from invariance of the Hamiltonian under mirror permutations of particles, (2.27), and

$$q_k \leftrightarrow \bar{q}_k \quad (4.11)$$

which is connected with the symmetry under interchange of the z - and \bar{z} -sectors. Therefore, the four points, *i.e.* $\{q_k\}$, $\{(-1)^k q_k\}$, $\{q_k^*\}$ and $\{(-1)^k q_k^*\}$ with $k = 2, \dots, N$, are related and all of them satisfy the quantization conditions (3.28), (3.29) and have the same energy.

4.4. Descendent states

Let us first discuss the spectrum along the trajectories with the highest conformal charge q_N equal zero for arbitrary $\nu_h \in \mathbb{R}$. It turns out [29, 26, 27, 23] that the wave-functions of these states are built of $(N-1)$ -particle states. Moreover, their energies [41] are also equal to the energy of the ancestor $(N-1)$ -particle states:

$$E_N(q_2, q_3, \dots, q_N = 0) = E_{N-1}(q_2, q_3, \dots, q_{N-1}). \quad (4.12)$$

Thus, we call them the descendent states of the $(N-1)$ -particle states.

Generally, for odd N , the descendent state $\Psi_N^{(q_N=0)}$ with the minimal energy $E_N(q_N = 0) = 0$ has for $q_2 = 0$, (*i.e.* for $h = 0, 1$), the remaining

integrals of motion $q_3 = \dots = q_N = 0$ as well. For $h = 1 + i\nu_h$, *i.e.* $q_2 \neq 0$, the odd conformal charges $q_{2k+1} = 0$ with $k = 1, \dots, (N-1)/2$ while the even ones $q_{2k} \neq 0$ and depend on ν_h .

On the other hand, for even N , the eigenstate with the minimal energy $\Psi_N^{(q_N=0)}$ is the descendent state of the $(N-1)$ -particle state which has minimal energy with $q_{N-1} \neq 0$. Thus, $E_N^{min}(q_N = 0) = E_{N-1}^{min}(q_{N-1} \neq 0) > 0$.

Studying more thoroughly this problem one can obtain [29, 23] a relation between the quasimomentum θ_N of the descendent state and the ancestor one θ_{N-1} , which takes the following form

$$e^{i\theta_N} \Big|_{q_N=0} = -e^{i\theta_{N-1}} = (-1)^{N+1}. \quad (4.13)$$

Additionally, one can define a linear operator Δ [29, 23] that maps the subspace $V_{N-1}^{(q_{N-1})}$ of the $(N-1)$ -particle ancestor eigenstates with the quasimomentum $\theta_{N-1} = \pi N$ into the N -particle descendent states with $q_N = 0$ and $\theta_N = \pi(N+1)$ as

$$\Delta : V_{N-1}^{(\theta_{N-1}=\pi N)} \rightarrow V_N^{(\theta_N=\pi(N+1))}. \quad (4.14)$$

It turns out that this operator is nilpotent for the eigenstates which form trajectories [29], *i.e.* $\Delta^2\Psi = 0$. Thus, the descendent-state trajectory can not be ancestor trajectory for $(N+1)$ -particle states. However, it is possible to build a single state [23] with $q_2 = q_3 = \dots = q_N = 0$, *i.e.* for only one point $\nu_h = 0$, that has $E_N = 0$ and the eigenvalue of Baxter Q -operator defined as

$$Q_N^{q=0}(u, \bar{u}) \sim \frac{u - \bar{u}}{\bar{u}^N}, \quad (4.15)$$

where a normalization factor was omitted. For $N = 3$ this state corresponds to the wave-function defined in (3.38).

Additional examples of the descendent states for $N = 3$ will be described later in the next sections.

5. Numerical results

5.1. Quantum numbers of the $N = 3$ states

In this section we present the spectrum of q_3 for three reggeized gluons. For the first time such solutions for $\text{Re}[q_3] = 0$ were obtained in [40]. The authors of Ref. [40] used the method of the \hat{q}_3 eigenfunctions described in Section 5. Similar quantization condition was also constructed in [26]. Solutions with $\text{Re}[q_3] \neq 0$ were found in [37, 38]. Moreover, in the latter paper the solutions with $n_h \neq 0$ are described.

The first solution using the Baxter Q -operator method was described in Ref. [23]. Later, similar results were also obtained in Ref. [25]. It turns out that the Baxter Q -operator method [23] for $N = 3$ is equivalent to the method of the \hat{q}_3 eigenfunctions described in Section 5. For higher $N > 3$ only the Baxter Q -operator method was used to find the quantization values of q_N and the energy.

5.2. Lattice structure

Solving the quantization conditions (3.28) and (3.29) for $N = 3$ and for $h = \frac{1+n_h}{2}$, *i.e.* with $\nu_h = 0$, we reconstruct the full spectrum of q_3 . It is convenient to show the spectrum in terms of $q_3^{1/3}$ rather than q_3 . Since $q_3^{1/3}$ is a multi-valued function of complex q_3 , each eigenstate is represented on the complex $q_3^{1/3}$ -plane by $N = 3$ different points. Thus, the spectrum is symmetric under the transformation

$$q_3^{1/3} \leftrightarrow \exp(2\pi ik/3)q_3^{1/3}, \quad \text{where } 0 < k < 3. \quad (5.1)$$

Additionally, mirror symmetry (4.10) results in a more regular structure. For the total $\text{SL}(2, \mathbb{C})$ spin of the system $h = 1/2$, which means $n_h = 0$ and $\nu_h = 0$, we present the spectrum in Fig. 1. One can easily notice that

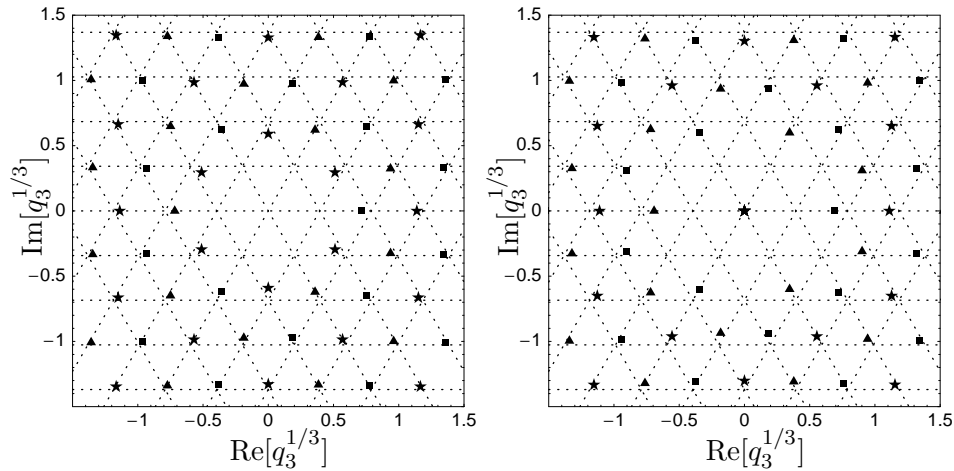


Figure 1. The spectrum of quantized $q_3^{1/3}$ for the system of $N = 3$ particles. On the left the total $\text{SL}(2, \mathbb{C})$ spin of the system is equal to $h = \frac{1}{2}$, while on the right $h = 1$. Different symbols stand for different quasimomenta θ_3 : stars $\theta_3 = 0$ boxes $\theta_3 = 4\pi/3$ triangles $\theta_3 = 2\pi/3$.

the spectrum has the structure close to the equilateral triangle lattice of the

leading order WKB approximation (5.8). Indeed, apart from a few points close to the origin, the quantized values of $q_3^{1/3}$ are located almost exactly at the vertices of the WKB lattice. The WKB formula [21] gives

$$[q_3^{\text{WKB}}(\ell_1, \ell_2)]^{1/3} = \Delta_{N=3} \left(\frac{1}{2}\ell_1 + i\frac{\sqrt{3}}{2}\ell_2 \right), \quad (5.2)$$

where ℓ_1 and ℓ_2 are integers, such that their sum $\ell_1 + \ell_2$ is even. Here the lattice spacing is denoted by

$$\Delta_3 = \left[\frac{3}{4^{1/3}\pi} \int_{-\infty}^1 \frac{dx}{\sqrt{1-x^3}} \right]^{-1} = \frac{\Gamma^3(2/3)}{2\pi} = 0.395175\dots \quad (5.3)$$

The lattice of $q_3^{1/3}$ extends onto the whole complex plane except the interior of the disk with the radius Δ_3 :

$$|q_3^{1/3}| > \Delta_3 \quad (5.4)$$

situated at $q_3 = 0$.

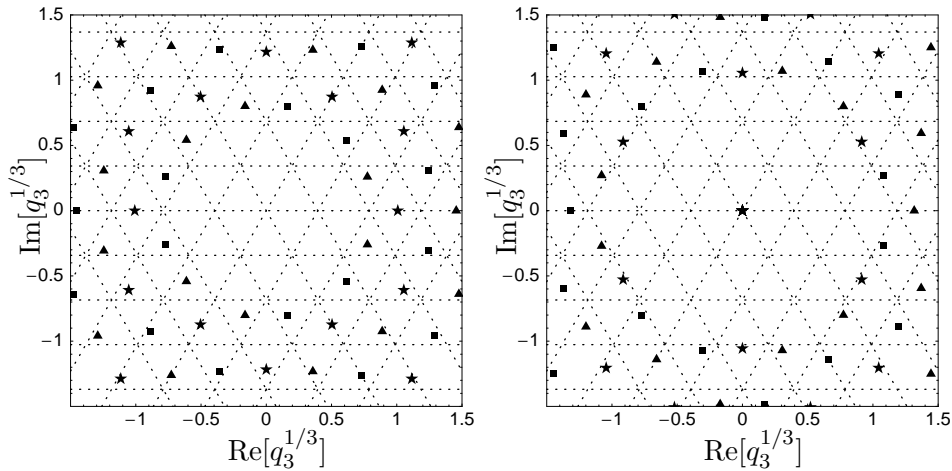


Figure 2. The spectrum of quantized $q_3^{1/3}$ for the system of $N = 3$ particles. On the left the total $\text{SL}(2, \mathbb{C})$ spin of the system is equal to $h = \frac{3}{2}$, while on the right $h = 2$. Different symbols stand for different quasimomenta θ_3 : stars $\theta_3 = 0$ boxes $\theta_3 = 4\pi/3$ triangles $\theta_3 = 2\pi/3$.

In accordance with (5.2), a pair of integers ℓ_1 and ℓ_2 parameterize the quantized values of $q_3^{1/3}$. Going further, one can calculate the quasimomen-

tum as a function of ℓ_1 and ℓ_2 . It has a following form

$$\theta_3(\ell_1, \ell_2) = \frac{2\pi}{3}\ell_1 \pmod{2\pi}. \quad (5.5)$$

Thus, as we can see states with the same value of $\text{Re}[q_3^{1/3}]$ have the same quasimomentum. In Fig. 1, different quasimomenta are distinguished by *stars*, *boxes* and *triangles*.

The same lattice structure is exhibited by the spectra with different n_h . However, they have different corrections to the leading order WKB approximation for $q_3^{1/3}$. These spectra are presented in Figs.1-2. The corrections to the lattice structure depend on q_2 as seen in (5.8). Since the WKB lattice is obtained in the leading order of the expansion for large conformal charges, $1 \ll |q_2^{1/2}| \ll |q_3^{1/3}|$, the corrections are bigger for lower $|q_3^{1/3}|$. Later, we shall discuss some other features of the corrections to the WKB leading order approximation.

As we can see in Figs. 1-2 for $h \in \mathbb{Z}$ we have additionally trajectories with $q_3 = 0$. They are called the descendent states because their spectra are related to the spectra for the $N - 1 = 2$ Reggeon states. We discuss this point further below.

5.3. Trajectories in ν_h

In the previous Section we considered the dependence of q_3 on n_h for $\nu_h = 0$. However, the spectrum of conformal charges also depends on the continuous parameter ν_h with $h = \frac{1+n_h}{2} + i\nu_h$. It turns out that the spectrum is built of trajectories parameterized by real parameter ν_h . Each trajectory crosses one point (*star*, *box*, *triangle*) in Figs. 1-2. An example of three such trajectories is presented in Fig. 3. They are numbered by $(\ell_1, \ell_2) = (0, 2)$, $(2, 2)$ and $(4, 2)$ whereas they quasimomentum $\theta_3(\ell_1, \ell_2) = 0, 4\pi/3$ and $2\pi/2$, respectively.

The trajectories cumulate at $\nu_h = 0$. When we increase ν_h , $q_3^{1/3}$ tends to infinity and the structure of quantized charges starts to be less regular, especially for trajectories with lower $|q_3^{1/3}|$. We can see this in Fig. 4 where we project trajectories with $h = \frac{1}{2} + i\nu_h$ on the $\nu_h = 0$ plane. Here *stars* denote point with $\nu_h = 0$, *boxes* with $\nu_h = 1$ and *circles* $\nu_h = 2$. Grey lines are drawn to show the projection of the trajectories for intermediate values of ν_h .

For $n_h \neq 0$ we notice that the spectra start to rotate with ν_h . In Fig. 4 and 5 we present trajectories with positive $n_h = 0, 1, 2, 3$. Due to the symmetry (4.11), which means $h \rightarrow 1 - h^*$ or $n_h \rightarrow -n_h$ with $q_3 \rightarrow q_3^*$, or equivalently, $\nu_h \rightarrow -\nu_h$ but $q_3 \rightarrow q_3$, the spectrum for the negative n_h is the

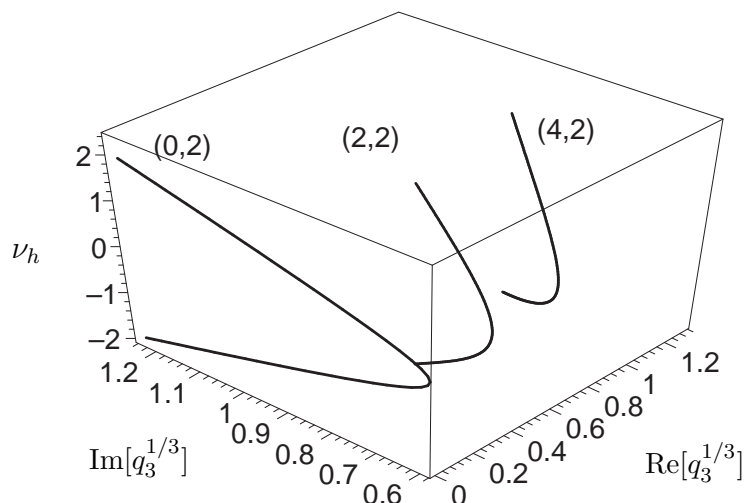


Figure 3. The dependence of quantized $q_3(\nu_h; \ell_1, \ell_2)$ on the total spin $h = 1/2 + i\nu_h$. Three curves correspond to the trajectories with $(\ell_1, \ell_2) = (0, 2), (2, 2)$ and $(4, 2)$.

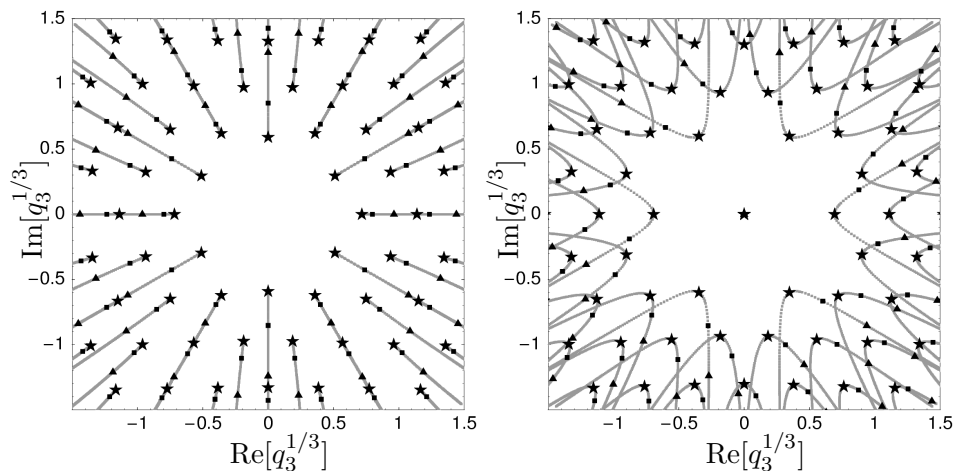


Figure 4. The trajectories of $q_3^{1/3}$ projected on $\nu_h = 0$. On the left panel $h = \frac{1}{2} + i\nu_h$, while on the right one $h = 1 + i\nu_h$. stars denotes $\nu_h = 0$, boxes $\nu_h = 1$ and triangles $\nu_h = 2$.

same as for the positive ones but it rotates in the opposite direction with ν_h .

Some of the results presented in this Section were found in earlier works [36, 38]. Trajectories with quasimomentum $\theta_3 = 0$ and $n_h = 0$ were obtained

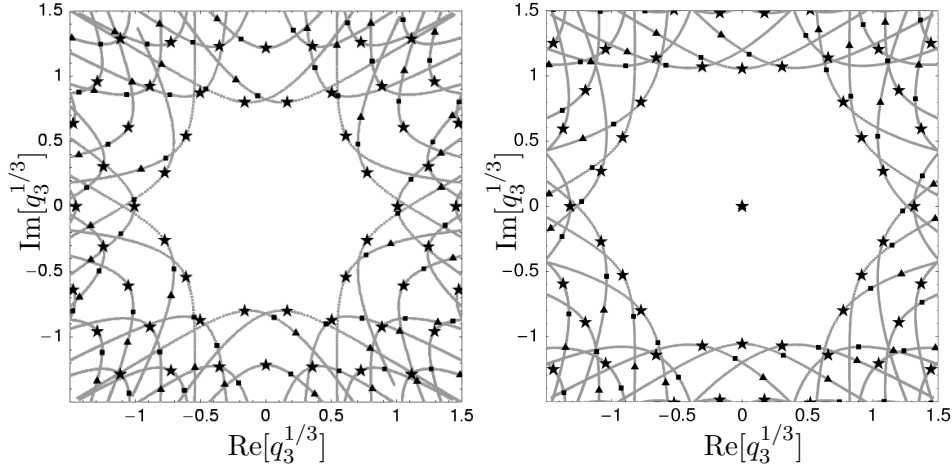


Figure 5. The trajectories of $q_3^{1/3}$ projected on $\nu_h = 0$. On the left panel $h = \frac{3}{2} + i\nu_h$, while on the right one $h = 2 + i\nu_h$. *stars* denotes $\nu_h = 0$, *boxes* $\nu_h = 1$ and *triangles* $\nu_h = 2$.

in Refs. [36, 38]. The case for $h = 2 + i\nu_h$ with quasimomentum $\theta_3 = 0$ was discussed in Ref. [38]. In this work we additionally analyse the spectra for $h = 1 + i\nu_h$ and $h = 3/2 + i\nu_h$.

5.4. Energy and dispersion

For all trajectories in (q_2, q_3) -space we can calculate the energy of the reggeized gluons using Eq. (4.4). Example of the energy spectrum for trajectories from Fig. 3 with $h = \frac{1}{2} + i\nu_h$ is shown in Fig. 6.

The energy along the trajectories is a continuous gapless function of ν_h . As we can see the energy E_3 grows with rising $|\nu_h|$. For $n_h = 0$ it has a minimum value $\min_{\nu_h} E_3(\nu_h; \ell_1, \ell_2)$ at $\nu_h = 0$. In the case $n_h \neq 0$, due the bending of the trajectories some minima of the energy are moved away from $\nu_h = 0$ [38]. However, the ground state corresponds to the point(s) on the plane of $q_3^{1/3}$ (see Fig. 1) closest to the origin. For $N = 3$ the ground state is located on the $(0, 2)$ -trajectory at $\nu_h = 0$ and $n_h = 0$ with quasimomentum equal $\theta_3 = 0$. Due to the symmetry (4.10) it is doubly-degenerated and its conformal charge and energy take the following values:

$$iq_3^{\text{ground}} = \pm 0.20526\dots, \quad E_3^{\text{ground}} = 0.98868\dots \quad (5.6)$$

In the vicinity of $\nu_h = 0$ the accumulation of the energy levels is described by the dispersion parameter (4.8) $\sigma_3 = 0.9082$.

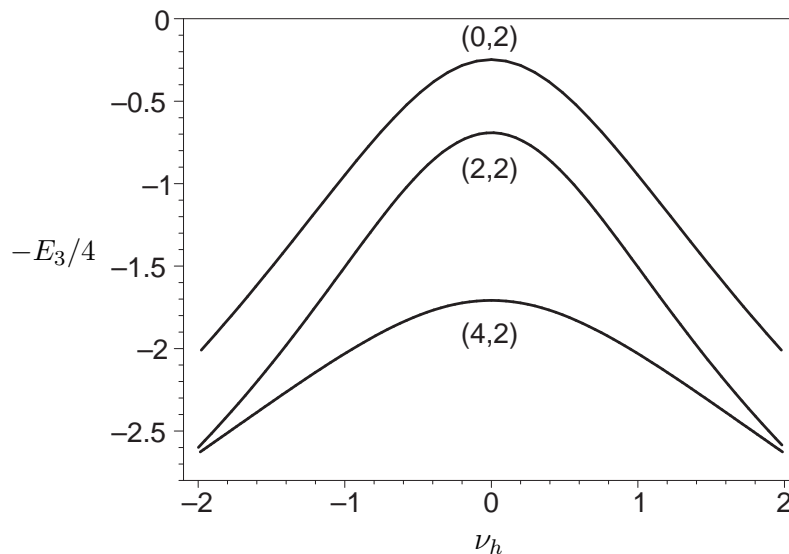


Figure 6. The energy spectrum corresponding to three trajectories shown in Fig. 3. The ground state is located on the $(0, 2)$ -trajectory at $\nu_h = 0$.

We show comparison of the WKB result of Eq. (5.2) with the exact expressions for q_3 at $h = 1/2$ in Fig. 1 and Table 1. One can find that the expression (5.2) describes the excited eigenstates with good accuracy. In the case where the eigenstates have smaller q_3 agreement becomes less accurate. Thus, for the ground state with $i q_3 = 0.20526 \dots$ the accuracy of (5.2) is $\sim 20\%$. Obviously, in the region where the WKB expansion is valid, *i.e.* $|q_3^{1/3}| \gg |q_2^{1/2}|$, Eq. (5.2) can be systematically improved by including subleading WKB corrections.

(ℓ_1, ℓ_2)	$(q_3^{\text{exact}})^{1/3}$	$(q_3^{\text{WKB}})^{1/3}$	$-E_3/4$
$(0, 2)$	$0.590 i$	$0.684 i$	-0.2472
$(2, 2)$	$0.358 + 0.621 i$	$0.395 + 0.684 i$	-0.6910
$(4, 2)$	$0.749 + 0.649 i$	$0.790 + 0.684 i$	-1.7080
$(6, 2)$	$1.150 + 0.664 i$	$1.186 + 0.684 i$	-2.5847
$(8, 2)$	$1.551 + 0.672 i$	$1.581 + 0.684 i$	-3.3073
$(10, 2)$	$1.951 + 0.676 i$	$1.976 + 0.684 i$	-3.9071

Table 1. Comparison of the exact spectrum of $q_3^{1/3}$ at $h = 1/2$ with the approximate WKB expression (5.2). The last line defines the corresponding energy $E_3(0; \ell_1, \ell_2)$.

5.5. Descendent states for $N = 3$

One also can notice in Figs. 4 and 5 that for odd n_h we have states with $q_3 = 0$. For $n_h = 0$ and $\nu_h = 0$ it has the energy $E_3 = 0$, so it is lower than (5.6). These states are descendants of the states with two Reggeons [26, 27, 28, 29, 23]. We constructed them in Section 3 using the \hat{q}_3 eigenfunction method. The wave-functions of these states are described by (3.31), (3.33), (3.38) and (3.40). These states have the same properties and the energy as the corresponding states with $N - 1 = 2$ particles, $E_3(q_2, q_3 = 0) = E_2(q_2)$, with [15, 16]:

$$\begin{aligned} E_2(q_2) &= 4 \operatorname{Re}[\psi(1 - h) + \psi(h) - 2\psi(1)] = \\ &= 8 \operatorname{Re} \left[\psi \left(\frac{1 + |n_h|}{2} + i\nu_h \right) - \psi(1) \right], \end{aligned} \quad (5.7)$$

where $\psi(x) = \frac{d}{dx} \ln \Gamma(x)$ and $q_2 = -h(h-1)$. Moreover, their wave-functions are built of the two-Reggeon states [29, 23] and the quasimomentum $\theta_3 = 0$. Contrary to the states with $q_3 \neq 0$, the states with $q_3 = 0$ (3.33) couple to a point-like hadronic impact factors [42, 43, 44], like the one for the $\gamma^* \rightarrow \eta_c$ transition.

5.6. Corrections to WKB

The WKB formula for the lattice structure of the conformal charge q_3 was derived in paper [21]. This formula tells us that for $q_3 \rightarrow \infty$

$$q_3^{1/3} = \frac{\Gamma^3(2/3)}{2\pi} \mathcal{Q}(\mathbf{n}) \left[1 + \frac{b}{|\mathcal{Q}(\mathbf{n})|^2} - \left(\frac{b}{|\mathcal{Q}(\mathbf{n})|^2} \right)^2 + \sum_{k=3}^{\infty} a_k \left(\frac{b}{|\mathcal{Q}(\mathbf{n})|^2} \right)^k \right], \quad (5.8)$$

where

$$\mathcal{Q}(\mathbf{n}) = \frac{1}{2}(l_1 + l_2) + i\frac{\sqrt{3}}{2}(l_1 - l_2) = \sum_{k=1}^3 n_k e^{i\pi(2k-1)/3} \quad (5.9)$$

and $l_1, l_2, \mathbf{n} = \{n_1, \dots, n_N\}$ are integers, while the coefficient

$$b = \frac{3\sqrt{3}}{2\pi} q_2^*, \quad (5.10)$$

where *star* denotes complex conjugation.

After numerical calculations we have noticed that better agreement with the exact results is obtained for

$$b = \frac{3\sqrt{3}}{2\pi} \left(q_2^* - \frac{2}{3} \right). \quad (5.11)$$

In order to show this, we calculated the values of the conformal charge q_3 for $h = \frac{1+n_h}{2}$ for $n_h = 0, 1, \dots, 19$. We evaluated numerically q_3 with $\text{Im}[q_3] = 0$, *i.e.* $a_k^{(r)}$, and separately with $\text{Re}[q_3] = 0$, *i.e.* $a_k^{(i)}$ where the superscript (i) and (r) refers to imaginary and real parts, respectively. Then we fitted expansion coefficients $a_k^{(r,i)}$ for large $|q_3|$ in the range $0 \dots 5000$ with high numerical precision. In order to save space in Table 2 we present results only for $n_h = 0, 1, 2$ and 3.

n_h	coef.	$k = 3$	$k = 4$	$k = 5$	$k = 6$	$k = 7$
0	$a_k^{(r)}$	0.509799695633	-10.065761318	-76.722084	-1508.927	-44580.
	$a_k^{(i)}$	3.490200304367	20.065761318	104.722084	-600.068	-40411.
	$a_k^{(r)} + a_k^{(i)}$	4.000000000000	10.0000000000	28.00000000	-2108.995	-84991.
1	$a_k^{(r)}$	-2.585231705744	-34.383865187	-209.366287	-1828.065	-26404.
	$a_k^{(i)}$	6.585231705744	44.383865187	237.366287	340.913	-16641.
	$a_k^{(r)} + a_k^{(i)}$	4.000000000000	10.0000000000	28.00000000	-1487.152	-43046.
2	$a_k^{(r)}$	1.336317342408	1.2054728742	-3.08256385	-31.51219	-196.87
	$a_k^{(i)}$	2.663682657592	8.7945271258	31.08256385	110.89046	377.64
	$a_k^{(r)} + a_k^{(i)}$	4.000000000000	10.0000000000	28.00000000	79.37827	180.77
3	$a_k^{(r)}$	2.250754858908	6.7220206127	22.76106772	79.325249	268.13
	$a_k^{(i)}$	1.749245141092	3.2779793873	5.23893228	-0.430149	-75.81
	$a_k^{(r)} + a_k^{(i)}$	4.000000000000	10.0000000000	28.00000000	78.895100	192.32

Table 2. The fitted coefficient to the series formula of $q_3^{1/3}$ (5.8) with $n_h = 0, 1, 2$ and 4

Coefficients a_k for $k = 0, \dots, 2$ agree with formula (5.8), *i.e.* $a_0 = 1$, $a_1 = 1$ and $a_2 = -1$, but as we previously mentioned in (5.10) and (5.11), the expansion parameter $b/|\mathcal{Q}(\mathbf{n})|^2$ is different. This difference comes from the fact that the series formula (5.8) with (5.10) is derived in the limit $1 \ll |q_2^{1/2}| \ll |q_3^{1/3}|$. Since in (5.11) the value of q_2^* is much bigger than $2/3$ the value of the parameter b from (5.11) in the above limit goes to (5.10). One may suppose therefore that the factor $2/3$ in Eq. (5.11) as subleading was omitted in the derivation presented in Ref. [21].

Secondly, we see that the coefficients a_k with $k > 2$ start to depend on n_h . Thus, to describe the behaviour of $q_3^{1/3}$ properly, we have to introduce a second expansion parameter, for example q_2 . We can also notice that for $k > 2$ for a few first coefficients $a_k^{(i)} + a_k^{(r)} \in \mathbb{Z}$ and this sum does not depend on n_h .

Moreover, we can see that after the numerical fitting we obtain two different sets of the expansion coefficients, $\{a_k^{(r)}\}$ and $\{a_k^{(i)}\}$, defined in (5.8), for real and imaginary $q_3^{1/3}$, respectively. Thus, in order to describe full-

complex values of $q_3^{1/3}$ in terms of the series (5.8) we have to use both sets of coefficients, one for real and one for imaginary part of $q_3^{1/3}$. Alternatively, we can perform expansion with two small parameters, *i.e.* $q_2^*/|\mathcal{Q}(\mathbf{n})|^2$ and $1/|\mathcal{Q}(\mathbf{n})|^2$. Since the leading terms, *i.e.* with a_0 , a_1 and a_2 , for real and imaginary $q_3^{1/3}$ are equal and known analytically, good approximation is obtained using Eq. (5.8) with (5.11) and neglecting higher order terms with $a_{k \geq 3}$.

6. Summary

In this work we have considered the scattering processes in the Regge limit (2.1) where the compound reggeized gluon states, *i.e.* Reggeons, propagate in the t -channel and interact with each other. We have performed calculations in the generalized leading logarithm approximation (GLLA) [7, 8, 9], in which a number of Reggeons in the t -channel is constant. We attempted to find a scattering amplitude of hadrons with multi-Reggeon exchange. However, a structure of reggeized gluon states as well as their properties have turned out to be so reach, complicated and interesting that in this work we have focused on description of the Reggeon state properties as well as on analysing the spectra of the energy and integrals of motion. The case for $N = 2$ reggeized gluons was calculated in Ref. [15, 16, 4]. Thus in this work we focused on $N = 3$ Reggeon states and dependence of their spectrum on conformal Lorentz spin n_h and scaling dimension $1+2\nu_h$ defined in (2.22).

In order to simplify the problem one applies the multi-colour limit [10], which makes the N -Reggeon system (2.10) $SL(2, \mathbb{C})$ symmetric (2.5) and completely integrable. In this limit the equation for the N -Reggeon wavefunction takes a form of Schrödinger equation (2.14) for the non-compact XXX Heisenberg magnet model of $SL(2, \mathbb{C})$ spins s [45, 46, 47]. Its Hamiltonian describes the nearest neighbour interaction of the Reggeons [13, 14] propagating in the two-dimensional transverse-coordinates space (2.5). The system has a hidden cyclic and mirror permutation symmetry (2.25). It also possesses the set of the $(N - 1)$ of integrals of motion, which are eigenvalues of conformal charges [33], \hat{q}_k and $\tilde{\hat{q}}_k$, (2.19)–(2.20). Therefore, the operators of conformal charges commute with each other and with the Hamiltonian and they possess a common set of the eigenstates. However, for the $N = 3$ case the multi-colour limit does not change the Hamiltonian and its spectrum. We have the two integrals of motion \hat{q}_2 and \hat{q}_3 and additionally constant two-dimensional total momentum p .

Eigenvalues of the lowest conformal charge, q_2 , may be parameterized (2.21) by the complex spins s (2.7) and the conformal weight h , where h can be expressed by the integer Lorentz spin n_h and the real parameter ν_h related

to the scaling dimension (2.22). Solving the eigenequation for q_2 we have derived ansatzes for N -Reggeons states with an arbitrary number of Reggeons N as well as arbitrary complex spins s . Since the $N = 3$ Reggeon ansatz separates variables, the q_3 -eigenequation can be rewritten as a differential equation of a Fuchsian type with three singular points (3.4) [18]. We have solved this equation by a series method. Gluing solutions for different singular points, (3.9), (3.14) and (3.19), and taking care for normalization and single-valuedness of the Reggeon wave-function (3.8) we have obtained the quantization conditions (3.28)–(3.29) for integrals of motion ($q_2, \bar{q}_2, q_3, \bar{q}_3$) which we have solved numerically [23, 38]. For $q_3 = \bar{q}_3 = 0$ the series solutions have a simple form and we were able to resum them. Thus, we have obtained analytical expressions for the three-Reggeon wave-functions with $q_3 = 0$ (3.31)–(3.40).

In this work we have calculated the behaviour of the q_3 -spectrum for the conformal Lorentz spins $n_h = 0, 1, 2, 3$ and the scaling dimension $1 + 2i\nu_h$. Some results for $n_h > 0$ were presented before in Ref. [24] for $n_h = 1$ and Refs. [38] for $n_h = 3$. The quantized values of $q_3^{1/3}$ for given n_h and fixed ν_h exhibit the WKB lattice structure (5.2), which for $N=3$ takes a form an equilateral-triangle lattice (5.2), Figs. 1-5. The non-leading WKB corrections move the quantized value of q_3 away from the lattice and cause that the quantized values of q_3 lie outside a disk located around the origin of the lattice, *i.e.* near $q_3 = 0$. However, for odd n_h there exist states with $q_3 = 0$. They are called descendent states because their wave-functions are effectively built of $N = 2$ Reggeon states. The non-descendent state with the lowest energy belongs to $n_h = 0$ sector and its energy is positive (5.6). This state is double-degenerated and it appears to be the nearest one to the origin of the $q_3^{1/3}$ lattice. However, the ground state for $N = 3$ is the descendent one with $n_h = 1$ and energy $E_3 = 0$ (5.7). Having found the exact values of q_3 we are able to calculate corrections to the WKB approximation (5.11), Table 2. These corrections differ from the corrections obtained earlier in Ref. [21]. The difference seems to be caused by using only one expansion parameter η for two various conformal charges, q_2 and q_3 . The obtained corrections are subleading to the WKB approximation [21] which is an expansion for large values of conformal charges, *i.e.* $1 \ll |q_2^{1/2}| \ll |q_3^{1/3}|$.

The above calculations are of interest not only for perturbative QCD but also to statistical physics as the $SL(2, \mathbb{C})$ non-compact XXX Heisenberg spin magnet model [45, 46, 47]. This work opens the way for further studies related to the multi-Reggeon states as well as calculations of scattering amplitude for concrete processes.

Acknowledgements

I would like to warmly thank to Michał Przaszłowicz for fruitful discussions and help during writing this work. I am very grateful to G.P. Korchemsky, A.N.Manashov and S.É. Derkachov whom I worked in an early state of this project. I also thank to Jacek Wosiek for illuminating discussions. This work was supported by KBN PB 2-P03B-43-24, KBN PB 0349-P03-2004-27 and KBN PB P03B-024-27(2004-2007).

Appendix A

Conformal invariants and other variables

Let us consider a difference of coordinates $(z_1 - z_2)$. It changes under the $\text{SL}(2, \mathbb{C})$ transformation (2.5) as

$$(z'_1 - z'_2) = \left(\frac{az_1 + b}{cz_1 + d} - \frac{az_2 + b}{cz_2 + d} \right) = (cz_1 + d)^{-1}(cz_2 + d)^{-1}(z_1 - z_2). \quad (\text{A.1})$$

One can see that during the transformation (A.1) the factors $(cz_i + d)^{-1}$ appear in front of the difference. These factors also exist in the transformation law of the wave-function (2.23). In order to cancel these factors one can construct a fraction where the same additional factors appear in the denominator and numerator of the constructed fraction variable.

The fraction variable

$$x = \frac{(z_1 - z_2)(z_3 - z_0)}{(z_1 - z_0)(z_3 - z_2)} \equiv (z_1 z_2 z_3 z_0) \quad (\text{A.2})$$

is invariant under the $\text{SL}(2, \mathbb{C})$ transformations (2.5). There is only one independent invariant for four coordinates [34, 48]. One can see that the fractions coming from the $\text{SL}(2, \mathbb{C})$ transformation (A.1) cancel because

- the variable is a function of the coordinate differences (A.1),
- the coordinates in the numerator and denominator of the variable x are the same.

Therefore, simplifying the partial fractions we can obtain expression like $((az_i + b)(cz_j + d) - (az_j + b)(cz_i + d))$ which with making use of $ad - cb = 1$ goes to $(z_i - z_j)$. As we can see, we have to build $\text{SL}(2, \mathbb{C})$ -invariants from differences of the coordinates.

It is easy to see that performing permutations of coordinates we can construct six different dependent invariants

$$\begin{aligned} (z_1 z_2 z_3 z_0) &= x, & (z_3 z_2 z_1 z_0) &= 1/x, \\ (z_2 z_3 z_1 z_0) &= 1/(1-x), & (z_1 z_3 z_2 z_0) &= 1-x, \\ (z_3 z_1 z_2 z_0) &= (x-1)/x, & (z_2 z_1 z_3 z_0) &= x/(x-1). \end{aligned} \quad (\text{A.3})$$

Let us take another product of z_{ij}

$$\begin{aligned} w' &= \frac{(z'_1 - z'_2)}{(z'_1 - z'_0)(z'_2 - z'_0)} = (cz_0 + d)^2 \frac{(z_1 - z_2)}{(z_1 - z_0)(z_2 - z_0)} = \\ &= (cz_0 + d)^2 w. \end{aligned} \quad (\text{A.4})$$

One can see that since in the denominator we have two additional z_0 variables after the transformation we obtain a multiplying factor $(cz_0 + d)^2$. Similarly for w^h we obtain

$$w'^h = (cz_0 + d)^{2h} w^h. \quad (\text{A.5})$$

Now one can compare this transformation to the transformation of the $\text{SL}(2, \mathbb{C})$ wave-function (2.23).

For $N = 3$ the variables $w = \frac{(z_3 - z_2)}{(z_3 - z_0)(z_2 - z_0)}$ and $x = \frac{(z_1 - z_2)(z_3 - z_0)}{(z_1 - z_0)(z_3 - z_2)}$ transform under the cycling permutation (2.25) as

$$\begin{aligned} (x - 1) &\rightarrow \frac{(-x)}{(x - 1)} \rightarrow \frac{1}{(-x)} \rightarrow (x - 1), \\ (-x) &\rightarrow \frac{1}{(x - 1)} \rightarrow \frac{(x - 1)}{(-x)} \rightarrow (-x), \\ w &\rightarrow w(x - 1) \rightarrow w(-x) \rightarrow w \end{aligned} \quad (\text{A.6})$$

while under the mirror permutation:

$$\begin{aligned} (x - 1) &\rightarrow \frac{(x - 1)}{(-x)} \rightarrow (x - 1) \\ (-x) &\rightarrow \frac{1}{(-x)} \rightarrow (-x) \\ w &\rightarrow wx \rightarrow w \end{aligned} \quad (\text{A.7})$$

For higher N we have more invariants. All of them can be constructed [26] from

$$x_r = \frac{(z_{r-1} - z_r)(z_{r+1} - z_0)}{(z_{r-1} - z_0)(z_{r+1} - z_r)}; \quad \prod_{r=1}^N x_r = (-1)^N; \quad \sum_{r=1}^N (-1)^r \prod_{k=r+1}^N x_k = 0. \quad (\text{A.8})$$

Variables x_r are subject to the two conditions:

$$\prod_{r=1}^N x_r = (-1)^N \quad (\text{A.9})$$

and

$$\sum_{r=1}^N (-1)^r \prod_{k=r+1}^N x_k = 0. \quad (\text{A.10})$$

From (A.9) we have $x_1 = (-1)^N / \prod_{r=2}^N x_r$. From (A.10) we can calculate

$$x_2 = \frac{\sum_{r=2}^N (-1)^r \prod_{k=r+1}^N x_k}{\prod_{k=3}^N x_k}. \quad (\text{A.11})$$

Interchangeably, one can derive from (A.9) $x_N = (-1)^N / \prod_{r=1}^{N-1} x_r$ and next from (A.10)

$$x_{N-1} = \frac{(-1)^N}{\sum_{r=1}^{N-1} (-1)^r \prod_{k=r}^{N-2} x^k}. \quad (\text{A.12})$$

Thus, we see that we have for N particles $N - 2$ independent invariants built of the particle coordinates z_i .

Appendix B

Solutions for $N = 3$ and $s = 0$ around $x = 0^+$

The eigenequation for \hat{q}_3 (3.3) is a differential equation of the third order so around each singular point, $x = 0, 1, \infty$, it has three independent solutions. Around $x = 0^+$ we have an indicial equation

$$(h - n - r)(r + n - 1)(n + r) = 0, \quad (\text{B.1})$$

so its solutions are given by $r_1 = h$, $r_2 = 1$ and $r_3 = 0$. As we can see we have two cases when $h \notin \mathbb{Z}$ (one solution with $\text{Log}(x)$) and $h \in \mathbb{Z}$ (one solution with $\text{Log}(x)$ and one solution with $\text{Log}^2(x)$). As we will see below we also have to consider separately solutions with $q_3 = 0$.

Using the same method we can also found solutions around $x = 1$ and ∞ . However, to save the space we do not present them.

Appendix B.1 Solutions for $q_3 \neq 0$ and $h \notin \mathbb{Z}$

In the first case, *i.e.* for $h \notin \mathbb{Z}$ and $q_3 \neq 0$ the solutions look as follows

$$\begin{aligned} u_1(x) &= x^{r_1} \sum_{n=0}^{\infty} a_{n,r_1} x^n, \\ u_2(x) &= x^{r_2} \sum_{n=0}^{\infty} a_{n,r_2} x^n, \\ u_3(x) &= x^{r_3} \sum_{n=0}^{\infty} b_{n,r_3} x^n + x^{r_2} \sum_{n=0}^{\infty} a_{n,r_2} x^n \text{Log}(x), \end{aligned} \quad (\text{B.2})$$

where $a_{0,r}$ is arbitrary (*e.g.* equal to 1)

$$a_{1,r} = \frac{(iq_3 - (h - 2r)(h - r)r)}{(h - 1 - r)r(1 + r)} a_{0,r} \quad (\text{B.3})$$

and $m = n + r$

$$a_{n,r} = \frac{(h-m+1)(h-m+2)(m-2)}{(h-m)(m-1)m} a_{n-2,r} + \frac{(iq_3 - (1+h-m)(m-1)(h-2(m-1)))}{(h-m)(m-1)m} a_{n-1,r}, \quad (\text{B.4})$$

whereas $b_{0,r_3} = \frac{(h-1)}{iq_3} a_{0,r_2}$ and b_{1,r_3} is arbitrary. One can notice that coefficient b_{0,r_3} is well defined only for $q_3 \neq 0$. Moreover,

$$b_{2,r_3} = \frac{2 + (h-3)h - iq_3}{2(2-h)} b_{1,r_3} + \frac{3h-8}{2(2-h)} a_{1,r_3} + \frac{6+h(h-6)}{2(2-h)} a_{0,r_3} \quad (\text{B.5})$$

and

$$b_{n,r_3} = \frac{(h+1-m)(h-m+2)(m-2)}{(h-m)(m-1)m} b_{n-2,r_3} + \frac{iq_3 - (1+h-m)(m-1)(h-2(m-1))}{(h-m)(m-1)m} b_{n-1,r_3} + \frac{h^2 + h(7-4m) + (m-2)(3m-4)}{(h-m)(m-1)m} a_{n-3,r_3} - \frac{h^2 - 6h(m-1) + 6(m-1)^2}{(h-m)(m-1)m} a_{n-2,r_3} - \frac{2m - 3m^2 + h(2m-1)}{(h-m)(m-1)m} a_{n-1,r_3}, \quad (\text{B.6})$$

where $m = r_3 + n$.

Appendix B.2 Solution with $q_3 = 0$

In this case $a_{0,r}$ defined in (B.2) is arbitrary (*e.g.* equal to 1). For the first solution with $r_1 = h$ we have $a_{1,r_1} = 0$ whereas for the third one a_{1,r_3} is arbitrary (let us take 0). It turns out that we do not need Log-solutions. The second solution is more complicated. One can derive the exact formula for

$$a_{n,r_2} = a_{0,r_2} \prod_{k=1}^n \frac{k-h}{k+1} = \frac{\Gamma(1-h+n)}{\Gamma(1-h)\Gamma(n+2)} a_{0,r_2} \quad (\text{B.7})$$

and performing summations

$$\begin{aligned}
 u_1(x) &= x^{r_1} \sum_{n=0}^{\infty} a_{n,r_1} x^n = x^h a_{0,r_1}, \\
 u_2(x) &= x^{r_2} \sum_{n=0}^{\infty} a_{n,r_2} x^n = a_{0,r_2} x \sum_{n=0}^{\infty} \frac{\Gamma(1-h+n)}{\Gamma(1-h)\Gamma(n+2)} x^n = \\
 &= -a_{0,r_2} \frac{1}{h} ((1-x)^h - 1), \\
 u_3(x) &= x^{r_3} \sum_{n=0}^{\infty} a_{n,r_3} x^n = a_{0,r_3}. \tag{B.8}
 \end{aligned}$$

Gathering solutions (B.8) we have

$$u(x) = A + B(-x)^h + C(x-1)^h \tag{B.9}$$

where A, B, C are arbitrary. The above solution was presented by Lipatov and Vacca in Refs. [26, 29].

Appendix B.3 Solution with $q_3 \neq 0, q_2 = 0$ and $h = 1$

For $h = 0$, *i.e.* $q_2 = 0$, and $q_3 \neq 0$ we have a different set of solutions. Here we have three solutions of the indicial equation (B.1) which are integer $r_1 = 1, r_2 = 1, r_3 = 0$ so the solutions are given by

$$\begin{aligned}
 u_1(x) &= x^{r_1} \sum_{n=0}^{\infty} a_{n,r_1} x^n, \tag{B.10} \\
 u_2(x) &= x^{r_2} \sum_{n=0}^{\infty} b_{n,r_2} x^n + x^{r_1} \sum_{n=0}^{\infty} a_{n,r_1} x^n \text{Log}(x), \\
 u_3(x) &= x^{r_3} \sum_{n=0}^{\infty} c_{n,r_3} x^n + 2x^{r_2} \sum_{n=0}^{\infty} b_{n,r_2} x^n \text{Log}(x) + x^{r_1} \sum_{n=0}^{\infty} a_{n,r_1} x^n \text{Log}^2(x),
 \end{aligned}$$

where $a_{0,r}$ is arbitrary (*e.g.* equal 1)

$$a_{1,r} = \frac{r + r^2(2r - 3)}{r^2(1 + r) - iq_3} a_{0,r} \tag{B.11}$$

and $m = n + r$

$$a_{n,r} = -\frac{(m-3)(m-2)^2}{(m-1)^2 m} a_{n-2,r} + \frac{(m-2)(m-1)(2m-3) - iq_3}{(m-1)^2 m} a_{n-1,r}, \tag{B.12}$$

whereas

$$b_{1,r_2} = \frac{1}{2}(-iq_3 b_{0,r_2} + a_{0,r_1} - 5a_{1,r_1}) \quad (\text{B.13})$$

$$\begin{aligned} b_{n,r_2} = & -\frac{(n-1)^2(n-2)}{n^2(n+1)}b_{n-2,r_2} + \frac{(2m^3 - 3m^2 + m - iq_3)}{n^2(n+1)}b_{n-1,r_2} \\ & + \frac{1 + 6n(n-1)}{n^2(n+1)}a_{n-1,r_1} + \frac{(n-1)(5-3n)}{n^2(n+1)}a_{n-2,r_1} - \frac{(2+3n)}{n(n+1)}a_{n,r_1} \end{aligned} \quad (\text{B.14})$$

while $c_{0,r_3} = \frac{-2}{iq_3}a_{0,r_1}$, c_{1,r_3} is arbitrary and

$$c_{2,r_3} = -\frac{1}{2}iq_3 c_{1,r_3} + b_{0,r_2} - 5b_{1,r_2} + 3a_{0,r_1} - 4a_{1,r_1}, \quad (\text{B.15})$$

$$\begin{aligned} c_{n,r_3} = & -\frac{(n-2)^2(n-3)}{n(n-1)^2}c_{n-2,r_3} + \frac{-iq_3 - 6 + n(13 + n(2n-9))}{n(n-1)^2}c_{n-1,r_3} \\ & - \frac{2(n-2)(3n-8)}{n(n-1)^2}b_{n-2,r_2} + \frac{26 - 36n + 12n^2}{n(n-1)^2}b_{n-1,r_2} \\ & - \frac{6n^2 - 8n + 2}{n(n-1)^2}b_{n,r_2} + \frac{2(7-3n)}{n(n-1)^2}a_{n-3,r_1} - \frac{6(3-2n)}{n(n-1)^2}a_{n-2,r_1} \\ & + \frac{2(2-3n)}{n(n-1)^2}a_{n-1,r_1}. \end{aligned} \quad (\text{B.16})$$

Appendix B.4 Solution with $q_2 = q_3 = 0$ and $h = 1$

In this case $a_{0,r}$ is arbitrary (e.g. equal to 1). For the first solution with $r_1 = (h = 1)$ we have $a_{1,r_1} = 0$ and for the third one a_{1,r_3} with $r_3 = 0$ is arbitrary (let us take 0). The second solution is more complicated. We need Log-solutions

$$u_2(x) = x^{r_2} \sum_{n=0}^{\infty} b_{n,r_2} x^n + x^{r_1} \sum_{n=0}^{\infty} a_{n,r_1} x^n \text{Log}(x). \quad (\text{B.17})$$

Using recurrence relations with $b_{1,r_2} = \frac{1}{2}a_{0,r_1}$ (and $a_{n,r_1} = 0$ for $n > 0$)

$$\begin{aligned} b_{2,r_2} &= \frac{1}{3}b_{1,r_2}, \\ b_{n,r_2} &= -\frac{(n-1)^2(n-2)}{n^2(n+1)}b_{n-2,r_2} + \frac{(n-1)n(2n-1)}{n^2(n+1)}b_{n-1,r_2} \end{aligned} \quad (\text{B.18})$$

one can derive an exact formula for $b_{n,r_2} = b_{1,r_2} \frac{2}{(n+1)n}$ and performing summations with arbitrary $b_{0,r_2}(=0)$ we have $x \sum_{n=0}^{\infty} b_{n,r_2} x^n = 2b_{1,r_2}(x + \text{Log}(1-x) - x\text{Log}(1-x))$, so that

$$\begin{aligned} u_1(x) &= x^{r_1} \sum_{n=0}^{\infty} a_{n,r_1} x^n = a_{0,r_1} = xa_{0,r_1}, \\ u_2(x) &= a_{0,r_1}(x + \text{Log}(1-x) - x\text{Log}(1-x) + x\text{Log}(x)), \\ u_3(x) &= x^{r_3} \sum_{n=0}^{\infty} a_{n,r_3} x^n = a_{0,r_3}. \end{aligned} \quad (\text{B.19})$$

Gathering solutions (B.19) we have

$$u(x) = A + B(-x) + C((x-1)\text{Log}(x-1) + (-x)\text{Log}(-x)), \quad (\text{B.20})$$

where A, B, C are arbitrary. See also Ref. [24].

Appendix B.5 Solution with $q_3 \neq 0, q_2 = 0$ and $h = 0$

For $h = 0$, i.e. $q_2 = 0$, and arbitrary $q_3 \neq 0$ we have three solutions

$$\begin{aligned} u_1(x) &= x^{r_1} \sum_{n=0}^{\infty} a_{n,r_1} x^n \\ u_2(x) &= x^{r_2} \sum_{n=0}^{\infty} b_{n,r_2} x^n + x^{r_1} \sum_{n=0}^{\infty} a_{n,r_1} x^n \text{Log}(x) \\ u_3(x) &= x^{r_3} \sum_{n=0}^{\infty} c_{n,r_3} x^n + 2x^{r_2} \sum_{n=0}^{\infty} b_{n,r_2} x^n \text{Log}(x) + x^{r_1} \sum_{n=0}^{\infty} a_{n,r_1} x^n \text{Log}^2(x) \end{aligned} \quad (\text{B.21})$$

where $r_1 = 1, r_2 = 0$ and $r_3 = 0$. Here $a_{0,r}$ is arbitrary (e.g. 1)

$$a_{1,r} = \frac{-iq_3 + 2r^2}{r(1+r)^2} a_{0,r} \quad (\text{B.22})$$

and $m = n + r$

$$a_{n,r} = -\frac{(m-2)^2}{m^2} a_{n-2,r} + \frac{-iq_3 + 2(m-1)^3}{(m-1)m^2} a_{n-1,r}, \quad (\text{B.23})$$

whereas $b_{0,r_2} = -\frac{1}{iq_3} a_{0,r_1}$ and b_{1,r_2} is arbitrary while

$$b_{2,r_2} = \frac{1}{4}((2 - iq_3)b_{1,r_2} + 6a_{0,r_1} - 8a_{1,r_1}), \quad (\text{B.24})$$

$$\begin{aligned}
b_{n,r_2} &= -\frac{(n-2)^2}{n^2}b_{n-2,r_2} + \frac{-iq_3 + 2(n-1)^3}{n^2(n-1)}b_{n-1,r_2} \\
&\quad - \frac{(n-2)(3n-4)}{n^2(n-1)}a_{n-3,r_1} + \frac{6(n-1)}{n^2}a_{n-2,r_1} + \frac{2-3n}{n^2(n-1)}a_{n-1,r_1}. \quad (\text{B.25})
\end{aligned}$$

The coefficient $c_{0,r_3} = \frac{2}{iq_3}(2a_{0,r_1} + b_{1,r_2})$ and c_{1,r_3} is arbitrary and

$$c_{2,r_3} = \frac{1}{4}(2 - iq_3)c_{1,r_3} + 3b_{1,r_2} - 4b_{2,r_2} + 3a_{0,r_1} - \frac{5}{2}a_{1,r_1}, \quad (\text{B.26})$$

$$\begin{aligned}
c_{n,r_3} &= -\frac{(n-2)^2}{n^2}c_{n-2,r_3} + \frac{-iq_3 + 2(n-1)^3}{n^2(n-1)}c_{n-1,r_3} \\
&\quad - \frac{2(n-2)(3n-4)}{n^2(n-1)}b_{n-2,r_2} + \frac{12(n-1)}{n^2}b_{n-1,r_2} + \frac{2(2-3n)}{n(n-1)}b_{n,r_2} \\
&\quad + \frac{2(5-3n)}{n^2(n-1)}a_{n-3,r_1} + \frac{12}{n^2}a_{n-2,r_1} + \frac{2(1-3n)}{n^2(n-1)}a_{n-1,r_1}. \quad (\text{B.27})
\end{aligned}$$

Appendix B.6 Solution with $h = 0$ and $q_2 = q_3 = 0$

In this case $a_{0,r}$ is arbitrary. For the first solution with $r_1 = 1$ we have recurrence relations with $a_{1,r_1} = \frac{1}{2}a_{0,r_1}$

$$\begin{aligned}
a_{2,r_1} &= \frac{1}{3}a_{1,r_1}, \\
a_{n,r_1} &= -\frac{(n-1)^2}{n+1}a_{n-2,r_1} + \frac{2n^2}{n+1}a_{n-1,r_1}. \quad (\text{B.28})
\end{aligned}$$

Summing series up we derive an exact formula for

$$u_1(x) = x^{r_1} \sum_{n=0}^{\infty} a_{n,r_1} x^n = x \sum_{n=0}^{\infty} x^n a_{0,r_1} \frac{1}{n+1} = -\text{Log}(1-x). \quad (\text{B.29})$$

In the second solution, with $r_2 = 0$, we have arbitrary a_{1,r_2} (let us take 0) and solution is $u_2(x) = a_{0,r_2}$. The third one is with Log-solutions

$$u_3(x) = x^{r_3} \sum_{n=0}^{\infty} b_{n,r_3} x^n + x^{r_2} \sum_{n=0}^{\infty} a_{n,r_2} x^n \text{Log}(x). \quad (\text{B.30})$$

Using recurrence relations with arbitrary b_{0,r_3}

$$\begin{aligned}
b_{2,r_3} &= \frac{1}{2}b_{1,r_3} \\
b_{n,r_3} &= -\frac{(n-2)^3}{n^2}b_{n-2,r_3} + \frac{2(n-1)^2}{n^2}b_{n-1,r_3} \quad (\text{B.31})
\end{aligned}$$

one can derive an exact formula for $b_{n,r_3} = b_{1,r_3} \frac{1}{n}$ and performing summations with arbitrary $b_{0,r_3} (= 0)$ we have $\sum_{n=0}^{\infty} b_{n,r_3} x^n = -b_{0,r_3} \text{Log}(1-x)$. All these solutions look like

$$\begin{aligned} u_1(x) &= x^{r_1} \sum_{n=0}^{\infty} a_{n,r_1} x^n = -a_{1,r_3} \text{Log}(1-x), \\ u_2(x) &= x^{r_2} \sum_{n=0}^{\infty} a_{n,r_2} x^n = a_{0,r_2}, \\ u_3(x) &= x^{r_3} \sum_{n=0}^{\infty} b_{n,r_3} x^n + a_{0,r_2} \text{Log}(x) = -b_{0,r_3} \text{Log}(1-x) + a_{0,r_2} \text{Log}(x). \end{aligned} \quad (\text{B.32})$$

Gathering solutions (B.32) we obtain

$$u(x) = A + B \text{Log}(-x) + C \text{Log}(x-1), \quad (\text{B.33})$$

where A, B, C are arbitrary. See also Ref. [24].

Appendix B.7 Solution with $q_3 \neq 0$ and $h = 2$

For $h = 2$ and $q_3 \neq 0$ we have three solutions

$$\begin{aligned} u_1(x) &= x^{r_1} \sum_{n=0}^{\infty} a_{n,r_1} x^n, \\ u_2(x) &= x^{r_2} \sum_{n=0}^{\infty} b_{n,r_2} x^n + x^{r_1} \sum_{n=0}^{\infty} a_{n,r_1} x^n \text{Log}(x), \\ u_3(x) &= x^{r_3} \sum_{n=0}^{\infty} c_{n,r_3} x^n + 2x^{r_2} \sum_{n=0}^{\infty} b_{n,r_2} x^n \text{Log}(x) + x^{r_1} \sum_{n=0}^{\infty} a_{n,r_1} x^n \text{Log}^2(x) \end{aligned} \quad (\text{B.34})$$

with $r_1 = 2, r_2 = 1, r_3 = 0$. Here a_{0,r_1} is arbitrary (*e.g.* 1)

$$a_{1,r_1} = \frac{-iq_3 + 2r(r-1)(r-2)}{r(r^2-1)} a_{0,r_1} \quad (\text{B.35})$$

and $m = n + r_1$

$$a_{n,r_1} = -\frac{(m-3)(m-4)}{m(m-1)} a_{n-2,r_1} + \frac{-iq_3 + 2(m-1)(m-2)(m-3)}{(m-2)(m-1)m} a_{n-1,r_1}, \quad (\text{B.36})$$

whereas $b_{0,r_2} = -\frac{2}{iq_3} a_{0,r_1}$ and b_{1,r_2} is arbitrary while

$$b_{2,r_2} = \frac{1}{6} (-iq_3 b_{1,r_2} + 4a_{0,r_1} - 11a_{1,r_1}), \quad (\text{B.37})$$

$$\begin{aligned}
b_{n,r_2} = & -\frac{(n-2)(n-3)}{n(n+1)}b_{n-2,r_2} + \frac{-iq_3 + 2(n-2)(n-1)n}{n(n^2-1)}b_{n-1,r_2} \\
& - \frac{11 + 3(n-4)n}{n(n^2-1)}a_{n-3,r_1} + \frac{6(n-2)n+4}{n(n^2-1)}a_{n-2,r_1} \\
& + \frac{1-3n^2}{n(n^2-1)}a_{n-1,r_1}. \quad (\text{B.38})
\end{aligned}$$

Moreover, $c_{0,r_3} = \frac{2}{iq_3}b_{0,r_2}$ and $c_{1,r_3} = -\frac{4(b_{0,r_2}+b_{1,r_2})}{iq_3} - \frac{6a_{0,r_1}}{iq_3}$ and c_{2,r_3} is arbitrary while

$$c_{3,r_3} = \frac{1}{6}(-iq_3c_{2,r_3} + 2b_{0,r_2} + 8b_{1,r_2} - 22b_{2,r_2} + 12a_{0,r_1} - 12a_{1,r_1}), \quad (\text{B.39})$$

$$\begin{aligned}
c_{n,r_3} = & -\frac{(n-3)(n-4)}{n(n-1)}c_{n-2,r_3} + \frac{-iq_3 + 2(n-3)(n-2)(n-1)}{n(n-1)(n-2)}c_{n-1,r_3} \\
& + \frac{2(3n(6-n)-26)}{n(n-1)(n-2)}b_{n-3,r_2} + \frac{4(11-12m+3m^2)}{n(n-1)(n-2)}b_{n-2,r_2} \\
& - \frac{2(2-6m+3m^2)}{n(n-1)(n-2)}b_{n-1,r_2} - \frac{6(n-3)}{n(n-1)(n-2)}a_{n-4,r_1} \\
& + \frac{12}{n(n-1)}a_{n-3,r_1} - \frac{6}{n(n-2)}a_{n-2,r_1}. \quad (\text{B.40})
\end{aligned}$$

Appendix B.8 Solution with $q_3 = 0$ and $h = 2$

In this case $a_{0,r}$ is arbitrary (e.g. equal to 1). For the first solution with $r_1 = 2$ we have remaining coefficients $a_{n>0,r_1} = 0$. The second solution, with $r_2 = 1$, has an arbitrary a_{1,r_2} (we can take it as 0), $a_{2,r_2} = 0$ and third one with arbitrary a_{1,r_3}, a_{2,r_3} (we also set them to 0). All these solutions look like

$$\begin{aligned}
u_1(x) &= x^{r_1} \sum_{n=0}^{\infty} a_{n,r_1} x^n = x^2 a_{0,r_3}, \\
u_2(x) &= x^{r_2} \sum_{n=0}^{\infty} a_{n,r_2} x^n = x a_{0,r_2}, \\
u_3(x) &= x^{r_3} \sum_{n=0}^{\infty} a_{n,r_3} x^n = a_{0,r_3}. \quad (\text{B.41})
\end{aligned}$$

Gathering solutions (B.41) we have

$$u(x) = A + B(-x)^2 + C(x-1)^2, \quad (\text{B.42})$$

where A, B, C are arbitrary. As we can see this solution corresponds to the solution with $q_3 = 0$ and arbitrary $h \notin \{0, 1\}$. For other integer $h \notin \{0, 1\}$ we can observe the same correspondence.

References

- [1] M. Gell-Mann, M.L. Goldberger, F.E. Low, E. Marx, F.Zachariasen. Elementary particles of Conventional Field Theory as Regge poles. III. *Phys. Rev. B*, 133:145, 1964.
- [2] M. Gell-Mann, M.L. Goldberger, F.E. Low, E. Marx, F.Zachariasen. Elementary particles of Conventional Field Theory as Regge poles. IV. *Phys. Rev. B*, 133:161, 1964.
- [3] V. N. Gribov. A Reggeon diagram technique. *Sov. Phys. JETP*, 26:414–422, 1968.
- [4] V. S. Fadin, E. A. Kuraev, and L. N. Lipatov. On the Pomernanchuk singularity in asymptotically free theories. *Phys. Lett.*, B60:50–52, 1975.
- [5] J. Bartels. High-Energy behavior in a nonabelian gauge field theory. *Phys. Lett.*, B68:258, 1977.
- [6] H. Cheng and C. Y. Lo. High-energy amplitudes of Yang-Mills theory in arbitrary perturbative orders. 1. *Phys. Rev.*, D15:2959, 1977.
- [7] J. Bartels. High-energy behavior in a nonabelian gauge theory. 2. First corrections to $T(n \rightarrow m)$ beyond the leading $\ln s$ approximation. *Nucl. Phys.*, B175:365, 1980.
- [8] J. Kwiecinski and M. Praszalowicz. Three gluon integral equation and odd C singlet Regge singularities in QCD. *Phys. Lett.*, B94:413, 1980.
- [9] T. Jaroszewicz. Infrared divergences and Regge behavior in QCD. *Acta Phys. Polon.*, B11:965, 1980.
- [10] G. 't Hooft. A planar diagram theory for strong interactions. *Nucl. Phys.*, B72:461, 1974.
- [11] L. N. Lipatov. Pomeron and odderon in QCD and a two-dimensional conformal field theory. *Phys. Lett.*, B251:284–287, 1990.
- [12] L. N. Lipatov. High-energy asymptotics of multicolor QCD and two-dimensional conformal field theories. *Phys. Lett.*, B309:394–396, 1993.
- [13] L. N. Lipatov. High-energy asymptotics of multicolor qcd and exactly solvable lattice models. *JETP Lett.*, 59:596–599, 1994.
- [14] L. D. Faddeev and G. P. Korchemsky. High-energy QCD as a completely integrable model. *Phys. Lett.*, B342:311–322, 1995.
- [15] L. N. Lipatov I. I. Balitsky. The Pomernanchuk singularity in Quantum Chromodynamics. *Sov. J. Nucl. Phys.*, 28:822–829, 1978.
- [16] E. A. Kuraev, L. N. Lipatov, and V. S. Fadin. The Pomernanchuk singularity in nonabelian gauge theories. *Sov. Phys. JETP*, 45, 1977.

- [17] T. Jaroszewicz. High-energy multi - gluon exchange amplitudes. Triest preprint IC/80/175.
- [18] R. A. Janik and J. Wosiek. Solution of the odderon problem. *Phys. Rev. Lett.*, 82:1092–1095, 1999.
- [19] P. Gauron, B. Nicolescu, and L. Szymanowski. A possible field theoretical description of the odderon. IPNO/TH 87-53.
- [20] L. Lukaszuk and B. Nicolescu. A possible interpretation of p p rising total cross- sections. *Nuovo Cim. Lett.*, 8:405–413, 1973.
- [21] S. E. Derkachov, G. P. Korchemsky, and A. N. Manashov. Noncompact Heisenberg spin magnets from high-energy QCD. III: Quasiclassical approach. *Nucl. Phys.*, B661:533–576, 2003.
- [22] G. P. Korchemsky, J. Kotanski, and A. N. Manashov. Compound states of reggeized gluons in multi-colour QCD as ground states of noncompact Heisenberg magnet. *Phys. Rev. Lett.*, 88:122002, 2002.
- [23] S. E. Derkachov, G. P. Korchemsky, J. Kotanski, and A. N. Manashov. Noncompact Heisenberg spin magnets from high-energy QCD. II: Quantization conditions and energy spectrum. *Nucl. Phys.*, B645:237–297, 2002.
- [24] H. J. De Vega and L. N. Lipatov. Interaction of reggeized gluons in the Baxter-Sklyanin representation. *Phys. Rev.*, D64:114019, 2001.
- [25] H. J. De Vega and L. N. Lipatov. Exact resolution of the Baxter equation for reggeized gluon interactions. *Phys. Rev.*, D66:074013, 2002.
- [26] L. N. Lipatov. Duality symmetry of Reggeon interactions in multicolour QCD. *Nucl. Phys.*, B548:328–362, 1999.
- [27] J. Bartels, L. N. Lipatov, and G. P. Vacca. A new odderon solution in perturbative QCD. *Phys. Lett.*, B477:178–186, 2000.
- [28] J. Bartels, M. A. Braun, D. Colferai, and G. P. Vacca. Diffractive η_c photo- and electroproduction with the perturbative QCD odderon. *Eur. Phys. J.*, C20:323–331, 2001.
- [29] G. P. Vacca. Properties of a family of n reggeized gluon states in multicolour QCD. *Phys. Lett.*, B489:337–344, 2000.
- [30] Yu. V. Kovchegov, L. Szymanowski, and S. Wallon. Perturbative odderon in the dipole model. *Phys. Lett.*, B586:267–281, 2004.
- [31] R. J. Baxter. *Exactly Solved Models in Statistical Mechanics*. Academic Press, London, 1982.
- [32] M. A. Braun, P. Gauron, and B. Nicolescu. Direct calculations of the odderon intercept in the perturbative QCD. *Nucl. Phys.*, B542:329–345, 1999.
- [33] S. E. Derkachov, G. P. Korchemsky, and A. N. Manashov. Noncompact Heisenberg spin magnets from high-energy QCD. I: Baxter Q-operator and separation of variables. *Nucl. Phys.*, B617:375–440, 2001.
- [34] P. Di Francesco, P. Mathieu, D. Sénéchal. *Conformal Field Theory*. Springer, New York, 1982.
- [35] J. B. Zuber. An introduction to Conformal Field Theory. *Acta Phys. Polon.*, B26:1785–1813, 1995.

- [36] G. P. Korchemsky and J. Wosiek. New representation for the odderon wave function. *Phys. Lett.*, B464:101–110, 1999.
- [37] M. Praszalowicz and A. Rostworowski. Spectrum of the odderon charge for arbitrary conformal weights. *Acta Phys. Polon.*, B30:349–357, 1999.
- [38] J. Kotanski and M. Praszalowicz. Solutions of the quantization conditions for the odderon charge q_3 and conformal weight h . *Acta Phys. Polon.*, B33:657–682, 2002.
- [39] Jan Kotanski. Reggeized gluon states in Quantum Chromodynamics. 2005. The PhD Thesis, hep-th/0511279.
- [40] J. Wosiek and R. A. Janik. Solution of the odderon problem for arbitrary conformal weights. *Phys. Rev. Lett.*, 79:2935–2938, 1997.
- [41] G. P. Korchemsky. Bethe ansatz for QCD pomeron. *Nucl. Phys.*, B443:255–304, 1995.
- [42] R. Engel, D. Yu. Ivanov, R. Kirschner, and L. Szymanowski. Diffractive meson production from virtual photons with odd charge-parity exchange. *Eur. Phys. J.*, C4:93–99, 1998.
- [43] J. Czyzewski, J. Kwiecinski, L. Motyka, and M. Sadzikowski. Exclusive η_c photo- and electroproduction at HERA as a possible probe of the odderon singularity in QCD. *Phys. Lett.*, B398:400–406, 1997.
- [44] J. Bartels, M. A. Braun, and G. P. Vacca. The process $\gamma^* + p \rightarrow \eta_c + X$: A test for the perturbative QCD odderon. *Eur. Phys. J.*, C33:511–521, 2004.
- [45] L. A. Takhtajan and L. D. Faddeev. The quantum method of the inverse problem and the heisenberg xyz model. *Russ. Math. Surveys*, 34:11–68, 1979.
- [46] L. D. Faddeev, E. K. Sklyanin, and L. A. Takhtajan. The quantum inverse problem method. 1. *Theor. Math. Phys.*, 40:688–706, 1980.
- [47] N. M. Bogolyubov, A. G. Izergin, and V. E. Korepin. *Quantum inverse scattering method and correlation functions*. Univ. Press, Cambridge, 1993.
- [48] A. Staruszkiewicz. *Algebra i Geometria*. NKF, Kraków, 1993.